THE ANATOMICAL RECORD 303:1075–1103 (2020)

Vascular Patterns in the Heads of Dinosaurs: Evidence for Blood Vessels, Sites of Thermal Exchange, and Their Role in Physiological Thermoregulatory Strategies

WILLIAM RUGER PORTER* **AND LAWRENCE M. WITMER**
Department of Biomedical Sciences, Ohio University Heritage College of Osteopathic Medicine, Ohio Center for Ecology and Evolutionary Studies, Athens, Ohio

ABSTRACT

Body size has thermal repercussions that impact physiology. Large-bodied dinosaurs potentially retained heat to the point of reaching dangerous levels, whereas small dinosaurs shed heat relatively easily. Elevated body temperatures are known to have an adverse influence on neurosensory tissues and require physiological mechanisms for selective brain and eye temperature regulation. Vascular osteological correlates in fossil dinosaur skulls from multiple clades representing different body-size classes were identified and compared. Neurovascular canals were identified that differentiate thermoregulatory strategies involving three sites of evaporative cooling that are known in extant diapsids to function in selective brain temperature regulation. Small dinosaurs showed similarly sized canals, reflecting a plesiomorphic balanced pattern of blood supply and a distributed thermoregulatory strategy with little evidence of enhancement of any sites of thermal exchange. Large dinosaurs, however, showed a more unbalanced vascular pattern whereby certain sites of thermal exchange were emphasized for enhanced blood flow, reflecting a more focused thermal strategy. A quantitative, statistical analysis of canal cross-sectional area was conducted to test these anatomical results, confirming that large-bodied, and often large-headed, species showed focused thermal strategies with enhanced collateral blood flow to certain sites of heat exchange. Large theropods showed evidence for a plesiomorphic balanced blood flow pattern, yet evidence for vascularization of the large antorbital paranasal air sinus indicates theropods may have had a fourth site of heat exchange as part of a novel focused thermoregulatory strategy. Evidence presented here for differing thermoregulatory strategies based on size and phylogeny helps refine our knowledge of dinosaur physiology. Anat Rec, 303:1075–1103, 2020. © 2019 American Association for Anatomy

Key words: dinosaur; blood vessels; thermoregulatory strategy

Additional Supporting Information may be found in the online version of this article.

Grant sponsor: Jurassic Foundation Grant-in-aid of Research; Grant sponsor: National Science Foundation; Grant numbers: IOS-1050154, IOS-1456503, NSF IOB-0517257; Grant sponsor: Ohio Center for Ecology and Evolutionary Studies; Grant number: Research Fellowship; Grant sponsor: Ohio University; Grant numbers: Graduate Student Senate Grant-in-aid of Research, Student Enhancement Award; Grant sponsor: Sigma Xi; Grant number: Grant-in-aid of Research; Grant sponsor: University of California Welles Fund.

*Correspondence to: William Ruger Porter, Department of Biomedical Sciences, Ohio University Heritage College of Osteopathic Medicine, Ohio Center for Ecology and Evolutionary Studies, Athens, OH. E-mail: porterw1@ohio.edu

Received 28 June 2018; Revised 22 March 2019; Accepted 11 May 2019.

DOI: 10.1002/ar.24234
Published online 22 August 2019 in Wiley Online Library (wileyonlinelibrary.com).

INTRODUCTION

Thermoregulation is arguably one of the most important physiological processes to occur in the body. Maintaining body temperature within strict limits has direct interactions with metabolism (Tattersall et al., 2006; Gillooly, 2013), and protein conformation and efficiency (Guderley and Seebacher, 2011). Thermoregulation can occur via behavioral mechanisms (Cowles and Bogert, 1944), where the animal shifts body position or shuttles from a sunny area to shade, or via physiological mechanisms that use evaporative mechanisms to cool blood (Crawford et al., 1977; Dzialowski and O'Connor, 1999). The central nervous system is known to be sensitive to heat loads, and this temperature sensitivity is thought to induce respiratory responses (Tattersall et al., 2006). Diapsids are known to have specific thermoregulatory strategies that deploy cephalic sites of thermal exchange within respiratory airflow to maintain or influence head and brain temperature (Crawford et al., 1977; Tattersall et al., 2006). There are many publications that have pointed to the thermoregulatory ability of three sites—the oral, nasal, and orbital regions—to cool blood that is then shunted around neurosensory tissues to selectively regulate brain and eye temperatures (Crawford, 1977; Midtgård, 1984a; Spray and Belkin, 1973; Spotila et al., 1977; Borrell et al., 2005).

By examining extant taxa, we can easily detect differences in thermoregulatory strategies. For example, a turkey and a cormorant share broadly similar vascular patterns and have similar head sizes, but have very different proportions of blood flow to sites of thermal exchange (Porter and Witmer, 2016). Turkeys are large-bodied birds with roughly equivalent well-vascularized oral, nasal, and orbital regions. Cormorants, on the other hand, are underwater pursuit predators with reduced nasal regions and oral regions that lack a palatal plexus, yet demonstrate a well-vascularized orbital region. These two taxa have different thermoregulatory strategies: compared to turkeys which have a larger body mass and roughly equivalent blood supply to all three sites as part of what we regard here as a distributed thermoregulatory strategy, cormorants emphasize the orbital region as a site of thermal exchange and the other regions are reduced (Porter and Witmer, 2016) as part of a focused thermoregulatory strategy.

Nonavian dinosaurs (hereafter referred to simply as dinosaurs) exhibited a wide range of body sizes, and each size had clear thermal consequences. Large dinosaurs had a low surface-area-to-volume ratio that would have allowed their often immense bodies to absorb large amounts of heat from the environment but would have slowed the shedding of that heat. Arterial blood heated in the core would then have flowed forward to the head, potentially damaging the delicate brain and sense organs if the temperature of this core blood exceeded the physiological limits of those tissues. We thus might expect that this problem would have been ameliorated by efficient physiological mechanisms to buffer neurosensory tissues from elevated body temperatures. This study explored head vasculature in dinosaurs (Porter, 2015) and other diapsids (Porter and Witmer, 2015, 2016; Porter et al., 2016) to search for evidence of such mechanisms. A number of large-bodied dinosaurs exhibited enlarged narial regions to the point of occupying half of the skull length (e.g., sauropods, hadrosaurs, ceratopsids, and ankylosaurs), potentially indicating an emphasis on the physiological processes that occur within these regions (Witmer, 2001). Other regions of the head may similarly offer thermoregulatory opportunities, such as the oral cavity and orbital region.

A number of mathematical models have predicted dinosaur body temperatures (Seebacher et al., 1999; O'Connor and Dodson, 1999; Seebacher, 2003; Gillooly et al., 2006), indicating that large-bodied dinosaurs could have had elevated core body temperatures, easily attaining 35°C under normal circumstances (Seebacher, 2003; Eagle et al., 2011). Other studies have predicted core temperatures up to 48°C (Gillooly et al., 2006). Isotopic studies have indicated sauropod head temperatures were in the 36°C–38°C range, slightly cooler than some predicted body temperatures (Eagle et al., 2011), suggesting an ability to maintain a head-to-body temperature differential that is characteristic of extant diapsids (see Porter and Witmer, 2015, 2016; Porter et al., 2016, and references therein). For extant diapsids, lethal body temperatures among birds are typically above 37°C (Kendeigh, 1969), reaching as high as about 45°C in the desert-acclimated Bedouin fowl (Arad and Marder, 1982; Arad and Midtgård, 1984), whereas lethal temperatures for alligators (Colbert et al., 1946) and lizards (Tattersall et al., 2006) are about 39°C. Dinosaurs likely had similar ranges of lethal body temperatures, and based on isotopic and model data, some larger dinosaurs were likely near the upper thermal limit under certain conditions.

Small dinosaurs, on the other hand, had a higher surface-area-to-volume ratio that would have increased their ability to shed heat. Although small-bodied dinosaurs may have experienced times of heat stress, they also might have required physiological mechanisms to conserve or slow the shedding of heat, such as plesiomorphically retaining vascular structures that are just large enough to meet metabolic demands. Isotopic analyses on smaller dinosaurs showed body temperatures in the 33°C–38°C range (Eagle et al., 2011), and around 25°C for a 12 kg dinosaur, which is near ambient temperature (Gillooly et al., 2006).

Wheeler (1978) hypothesized that blood vessels would have presented a potential mechanism that dinosaurs used to influence head temperature. Wheeler (1978) did not test this hypothesis, and indeed there has not been much work published since that has probed dinosaur fossils for clues that would shed light on their thermoregulatory strategies.

This study was aided by our previous anatomical investigations of extant diapsids and vasculature within three known sites of thermal exchange, that is, the nasal, oral, and orbital regions (Porter, 2015; Porter and Witmer, 2015, 2016; Porter et al., 2016). By comparing the vasculature of extant species within these physiologically relevant sites of evaporative cooling, it was found that blood vessels can supply different amounts of blood (based on the size of the vessels) to different sites of thermal exchange. This finding highlights the differences between each species' thermoregulatory strategies. By extending this approach to investigations into the vasculature of nonavian dinosaurs, which have been shown to conform to broad diapsid vascular patterns (Porter, 2015), this study detected vascular osteological correlates that allowed the comparison of not only dinosaur vascular patterns, but also their thermoregulatory strategies.

New terminology was necessary to describe the results of this study. Species that did not emphasize any one particular site of thermal exchange over the others had a *distributed thermoregulatory strategy*, meaning that heat

exchange was distributed more or less equally across all three sites of thermal exchange as judged by vascular patterns. Species that emphasized one or more sites of thermal exchange had a *focused thermoregulatory strategy*, meaning one or two sites were primarily used in thermal exchange, again based on surface area and blood supply. Blood supply to these regions was determined by measuring bony canals that housed the anastomoses between the nasal, palatine, and maxillary vessels. When these three sets of canals were found to have similar relative diameters, the species was regarded as having a *balanced vascular pattern*, whereas when one or two sets of canals were larger relative to the others, the species was regarded as having an *unbalanced vascular pattern* (Fig. 1).

Most dinosaurs were found to conform to basic vascular and thermoregulatory patterns similar to their extant diapsid relatives (Fig. 2) by using blood vessels within the three known sites of thermal exchange. This study, however, detected a possible fourth site of heat exchange suggesting a novel focused thermoregulatory strategy in nonavian theropod dinosaurs. Nonavian theropods generally had a balanced blood supply pattern supporting a distributed thermoregulatory strategy when considering the three conventional sites of thermal exchange. Further investigation, however, revealed evidence for a vast blood supply to the region of the antorbital cavity, which in life housed the antorbital paranasal air sinus, indicating a novel focused thermoregulatory strategy. Because the

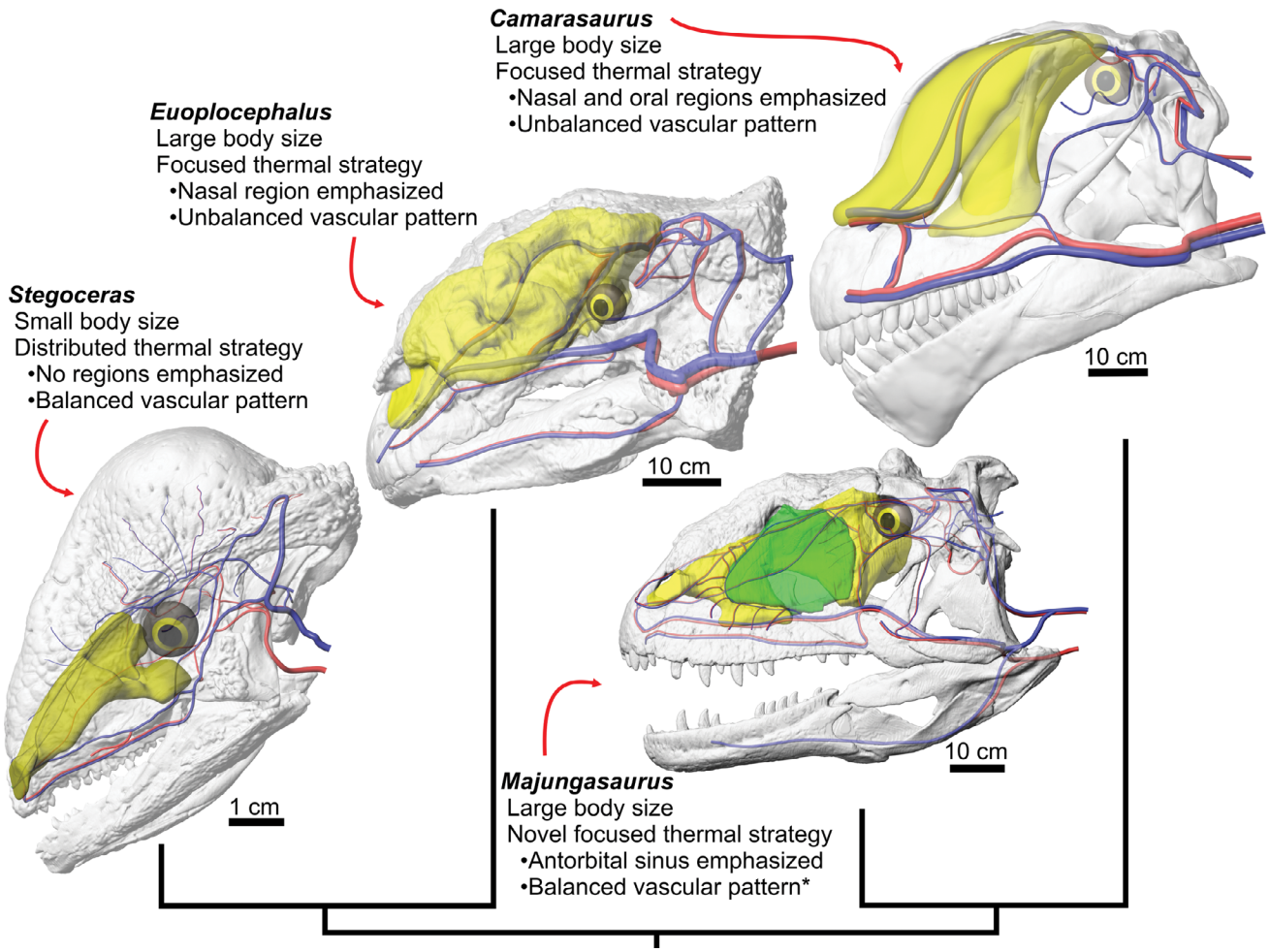

Fig. 1. *Stegoceras*, *Euoplocephalus*, *Majungasaurus*, and *Camarasaurus* in left lateral view showing the airway (yellow) and antorbital air sinus (green). As body sizes increased, the need for a thermoregulatory strategy to buffer neurosensory tissues from high heat loads increased. Each dinosaur species investigated showed a distributed or focused thermoregulatory strategy. A distributed thermoregulatory strategy distributes heat exchange to the orbital, oral, and nasal regions more or less equivalently. In species with a distributed thermoregulatory strategy (e.g., *Stegoceras*), the pattern of blood flow to the three main sites of thermal exchange observed in extant diapsids was considered balanced in that the sets of measured blood vessels in that species were roughly equivalent in size. In species with a focused thermoregulatory strategy (e.g., *Euoplocephalus* or *Camarasaurus*), one or two of the main sites of thermal exchange were emphasized with evidence for enhanced vascularization, leading to an unbalanced pattern of vascularization. This emphasized region was hypothesized to act as the principal site of thermal exchange. In the nonavian theropods (e.g., *Majungasaurus*), the large, actively ventilated antorbital paranasal air sinus within the antorbital cavity is hypothesized to be a novel kind of focused thermoregulatory strategy in that it does not involve in a major way any of the three main sites of thermal exchange observed in extant diapsids. In fact, the asterisk (*) designates that we found a balanced pattern of blood flow to the other three sites of thermal exchange, which is the plesiomorphic pattern typically found in small-bodied dinosaurs.

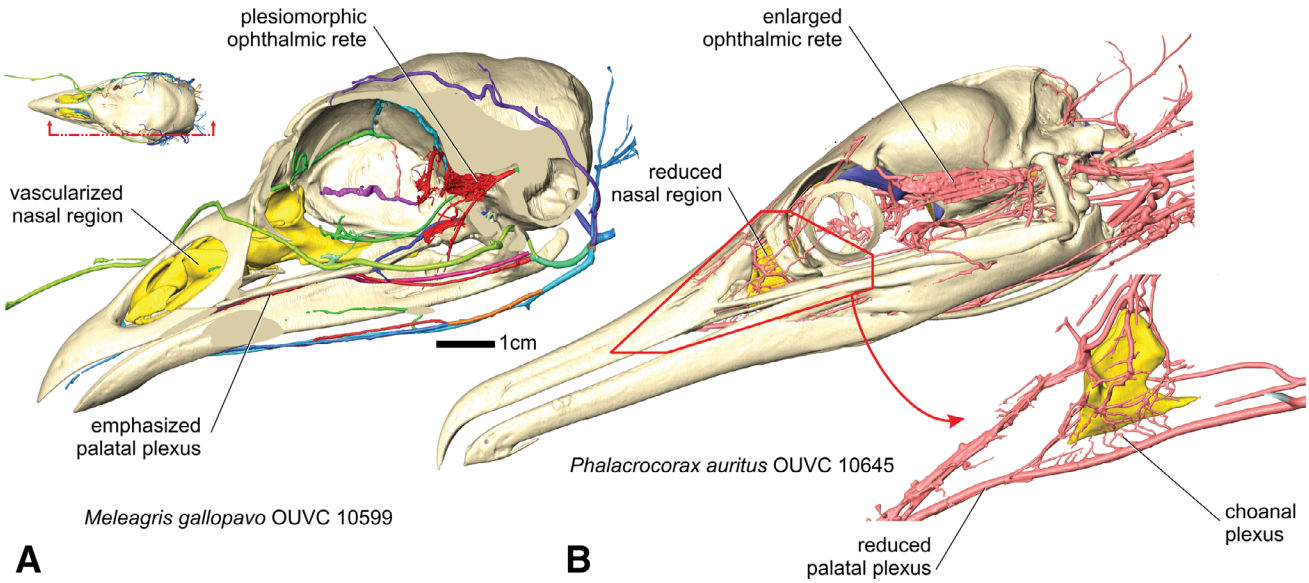

Fig. 2. Left lateral views of (**A**) *Meleagris gallopavo* (OUVC 10599) and (**B**) *Phalacrocorax auritus* (OUVC 10645). Comparisons of vascular anatomy in extant taxa revealed differential emphasis on each site of thermal exchange. A turkey (left) has a well-vascularized oral, nasal, and orbital region, and a cormorant (right) has a poorly vascularized oral and nasal region. The red box outlines the location of the nasal vasculature in the lower right corner. The orbital region of cormorants is well vascularized, indicating an emphasis placed on the blood vessels of the orbital region, and likely holds a prominent role in the cormorant thermoregulatory strategy.

blood vessels hypothesized to supply the antorbital sinus likely originated caudal to the measured anastomoses, this study did not detect a significant difference between the blood supplies to the three sites of thermal exchange and thus classified nonavian theropods as having balanced vascular patterns. By comparing the vasculature and thermoregulatory strategies of modern taxa (Fig. 2), we gain insight into similar physiological processes that dinosaurs would have used to thermoregulate and buffer temperatures of neurosensory tissues from heat loads that large body size would have incurred.

MATERIALS AND METHODS

Data Collection

Computed-tomography (CT) scans of extant specimens and small dinosaur fossils were acquired at the Ohio University μCT Scanning Facility on a GE eXplore Locus *in vivo* Small Animal MicroCT scanner at 45 and 90 μm slice thicknesses, 80 kV, 450 μA. Larger specimens were scanned at OhioHealth O'Bleness Hospital on a General Electric (GE) LightSpeed Ultra Multislice CT scanner equipped with the Extended Hounsfield option at 625 μm slice thickness, 120–140 kV, and 200–300 mA or a Toshiba Aquilion 64 CT scanner at 300 μm slice thickness, 120–140 kV, and 200–400 mA. CT scans allow for the visualization and 3D modeling of internal vascular osteological correlates of both extant and extinct taxa. Data acquired from CT scans were imported into and analyzed by the visualization software Avizo (ThermoScientific, Houston, TX) on a Dell T3400 Workstation with 8GB of RAM and an nVidia Quadro FX 4600 video card running Microsoft Windows 7 Enterprise. Datasets were scaled when necessary to conform to centimeter units.

The vascular or neurovascular canals of one gecko, one varanid, three iguanas (Porter and Witmer, 2016), six crocodilians (Porter et al., 2016), and 17 dinosaur skulls (Table 1) were digitally segmented and assigned to a material that was used to create a 3D surface. Birds were excluded from the quantitative part of this analysis due to a reduction of skull bones and the subsequent loss of most of the relevant vascular osteological correlates. The *Surface Cross-Section* tool in Avizo was used to create a zero-thickness slice of the segmented canal as close to perpendicular to the axis of the canal as feasible (Fig. 3). The area of this slice was measured, resulting in a two-dimensional cross-sectional area. Cross-sectional areas were collected for four canals (Table 1) that are known to convey blood vessels through the heads of extant diapsids: (1) cerebral carotid canal, (2) dorsal alveolar canal, (3) canal within the premaxilla that transmits branches of the nasal vessels, and (4) a canal in the maxilla or premaxilla that transmits branches of the palatine and lateral nasal vessels (Fig. 4). Canal cross-sectional area measurements were collected near the ventral aspect of the bony naris (Figs. 3 and 4) nearest to the canal foramen to capture the relationship of the palatine, dorsal alveolar, and nasal vessels as they anastomose within these canals (Porter and Witmer, 2015; Porter and Witmer, 2016; Porter et al., 2016). This position was chosen to reduce the influence of the larger, more caudal region of the neurovascular bundle because it supplies a wider range of tissues and regions, including the oral and nasal regions. This anastomosis (and hence the bony subnarial canal) is particularly important because it is hypothesized to act as a path of collateral blood flow to sites of thermal exchange (Porter, 2015). Therefore, as the narial or oral regions become enlarged for physiological reasons, blood supply is likely to increase beyond the minimum blood flow necessary to support the basic metabolism of the tissues within that region. Head volume was used as one measure of size, specifically to

TABLE 1. Untransformed cross-sectional areas (CSA) of cephalic vascular canals

Taxon	Dorsal alveolar (cm^2)	Palatal (cm^2)	Premaxillary (cm^2)	Cerebral carotid (cm^2)	Lateral nasal (cm^2)	Head volume (cm^3)	Estimated body mass (kg)
Alligator mississippiensis OUVC 9761	0.101	0.031	0.017	0.003	0.043	2,121.08	15.8[d]
Alligator mississippiensis OUVC 10615	0.143	0.060	0.053	0.037	0.111	4,628.92	33.6[d]
Alligator mississippiensis USNM 211233	0.188	0.138	0.062	0.148	0.408	13,067.00	116.3[d]
Camarasaurus CM 11338	0.508	0.479	0.144	0.106	1.112	2,983.07	3,838[a]
Camarasaurus GMNH PV 101 + UMNH VP 5665	–	4.325	–	0.262	4.659	35,149.07	18,174[a]
Crocodylus johnstoni OUVC 10426	0.007	0.001	0.002	0.008	0.003	64.66	1.44[a]
Crocodylus siamensis OUVC 11431	0.090	0.077	0.018	0.092	0.046	3,315.13	68.9[a]
Diplodocus CM 3452	0.316	1.966	0.237	0.241	3.638	4,198.37	14,813[a]
Diplodocus CM 11161	0.416	0.698	0.157	0.147	0.767	7,758.41	16,333[a]
Edmontonia AMNH 5381	0.318	0.274	0.417	0.479	0.430	8,158.37	1,530[a]
Euoplocephalus AMNH 5403	1.668	0.392	0.543	0.141	0.733	8,652.08	2,329[a]
Euoplocephalus AMNH 5405	2.501	0.435	1.053	0.365	2.607	9,500.72	2,329[a]
Gekko gecko OUVC 10870	0.0003	–	–	0.003	0.0003	7.54	0.04[c]
Iguana iguana OUVC 10603	0.007	0.002	0.004	0.003	–	27.63	0.78[e]
Iguana iguana OUVC 10611	0.017	0.005	0.004	0.004	0.013	57.21	0.94[a]
Iguana iguana OUVC 10612	0.006	0.004	0.003	0.006	0.006	7.40	0.81[e]
Majungasaurus FMNH PR 2100	0.169	–	0.242	0.164	–	15,606.29	1,614[a]
Panoplosaurus ROM 1215	0.273	0.576	0.295	0.385	0.116	5,192.73	1,372[a]
Pinacosaurus ZPAL MgD-II/1	0.144	0.064	–	0.072	0.057	1,065.48	–
Plateosaurus MB.R.1937	0.027	0.212	0.035	0.257	0.220	1,275.06	917[a]
Psittacosaurus MPC-D unnumbered	0.030	0.074	0.071	–	–	219.15	28[a]
Psittacosaurus IGM 100/1132	0.164	–	0.006	0.100	–	628.44	28[a]
Stegoceras UALVP 2	0.029	0.022	0.021	0.038	0.011	966.33	16[a]
Stegosaurus USNM 4934	0.070	–	0.185	0.587	–	2,637.42	4,869[a]
Tomistoma USNM 211322	0.346	0.027	0.043	0.113	0.184	15,082.40	350[d]
Tyrannosaurus rex BMR P2002.4.1	0.227	–	0.126	–	–	13,561.55	797[a]
Tyrannosaurus rex FMNH PR 2081 + AMNH 5117	2.086	2.163	0.430	0.141	2.048	214,915.92	6,403[a]
Varanus komodoensis TNHC 95803	0.014	0.052	0.040	0.065	0.037	1,076.54	75.6[b]

The dorsal alveolar canal is located within the maxilla, dorsal to the tooth row. The palatal canal is found within the suture between the maxilla and premaxilla (such as saurischian dinosaurs and crocodilians) or within the rostroventral premaxilla (such as ornithischian dinosaurs and iguana). The premaxillary canal is located within the dorsomedial aspect of the premaxilla, at the base of the nasal process. The cerebral carotid canal is found within the basisphenoid bone. The lateral nasal canals are variable, usually within the nasal bones or (usually hypermineralized) narial region. Head volume was calculated within Avizo. Spaces with a (–) represent missing data. A (+) indicates a composite was used. The carotid canal CSA for these specimens were measured from similarly sized fossils indicated by the number after the (+). Taxa are arranged in alphabetical order.

[a] Estimated using equations from Benson et al. (2018).
[b] Actual body mass.
[c] From Irschick et al. (1996).
[d] Estimated using equations from Edwards et al. (2017).
[e] Estimated using OUVC 10611 data.

control for the effects of head volume on canal size and because dinosaur body masses from the literature can vary widely even for the same specimen (Taylor, 2010; Campione and Evans, 2012). Head volume was measured from the same exact specimen as are the canal cross sections, removing error due to untested assumptions of intraspecific variation. Moreover, the cephalic blood vessels are supplying the head, not the body, and so head volume is a biologically relevant size metric, particularly given that species with similar body masses may have drastically different head shapes and sizes. Head volume (Table 1) was measured by segmenting CT data and wrapping the skull in a "skin" (the outer surface envelope of the head) and then subtracting the estimated volumes of the nasal and oral air spaces (Witmer and Ridgely, 2008; Snively et al., 2013). Diapsid 3D models (Porter and Witmer, 2015, 2016; Porter et al., 2016) made in Maya (Autodesk, San Rafael, CA) were used to visualize blood vessels. We also collected body-mass estimates from the literature (see Table 1) as another measure of body size. We then ran a partial least squares regression (PLS) and a phylogenetically informed principal components analysis (pPCA) to understand the effects of body-size parameters on the canal size, revealing the pressures to which blood vessels may have been responding, such as potentially the effects of high heat-loads induced by large body mass. The pPCA used residuals from a canal size versus head volume phylogenetically informed generalized least squares (pGLS) regression as a size-corrected estimate of the amount of blood required to support head tissue nutrition and metabolism. When head volume was controlled for, the remaining signal was interpreted as being independent of the blood supply necessary to maintain basic tissue nutritional requirements and thus reflects support for thermophysiological functions occurring in cephalic regions.

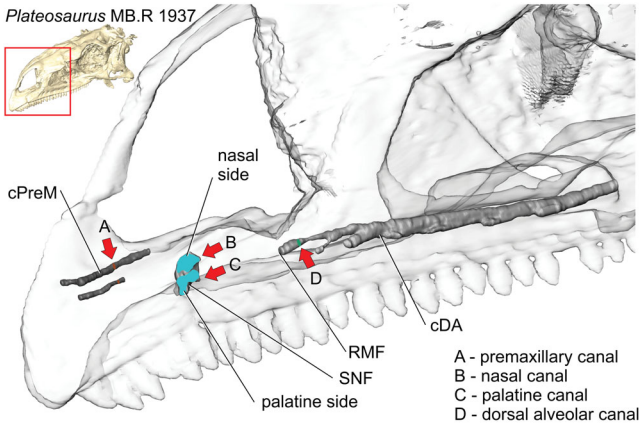

Fig. 3. *Plateosaurus* (MB.R.1937; basal sauropodomorph) demonstrating each segmented canal and its cross sectional area as measured in Avizo. Canals within the nasals, premaxilla, and maxilla were measured as a proxy for the size of the blood vessels within them. A though D indicate canals measured (key in lower left corner). Abbreviations: RMF, rostral maxillary foramen; cDA, dorsal alveolar canal; cPreM, premaxillary canals; SNF, subnarial foramen. Inset image indicates specimen orientation and red box indicates region of larger image.

Several studies have investigated canal or foramen diameters to assess their ability to predict the size of the artery, vein, or nerve within them (and hence predict some higher-order biological attribute such as a behavior). For example, Muchlinksi (2008) and Muchlinksi and Deane (2014) found that the infraorbital nerve foramen of primates contained large nerves and relatively small blood vessels. In a similar report, Jungers et al. (2003) investigated the hypoglossal canal in hominids, showing that the hypoglossal foramen was not a good predictor of nerve size as the foramen was filled with large blood vessels. In reptiles, Jamnickzy and Russell (2004) investigated turtle vascular canals by inputting the residuals from a generalized mean regression into a principal components analysis. The results indicated that the cerebral carotid artery contains enough data to be a sufficient character for turtle phylogenetic analyses. Barker et al. (2017) investigated similar canals in the maxilla and premaxilla of the theropod dinosaur *Neovenator* to explore maxillary neurovasculature and how it may have related to tactile abilities and ecomorphology, and reported that estimates of nerve size must be carefully considered. These reports show that canals and foramina can be analyzed as proxies for the soft tissues within them, if the ratio of nerve to blood vessel is known or at least approximated. The dinosaur study presented below likewise seeks to distinguish the main contents of canals and foramina, which indeed presents some challenges. In some cases (e.g., the subnarial foramen, the carotid canal, and the suborbital fenestra), there is little ambiguity because only blood vessels and no nerves traverse the aperture in extant diapsids, but in other cases the apertures are truly "neurovascular" and more caution must be exerted (see section on "Neurovascular canals" in Results). Nevertheless, given that a nerve, artery, and vein generally occupy neurovascular canals, our base assumption was that two-thirds of the canal contained blood vessels unless other evidence indicated otherwise.

Statistical Analysis

A phylogeny (Fig. 5) was constructed using existing topologies for node and crown taxa relationships (Butler et al., 2008; Hocknull et al., 2009; Heinicke et al., 2012; Thompson et al., 2012; Royo-Torres, 2014; Watanabe and Slice, 2014). Occurrence ranges were gathered from the literature (Table 2), and the R package STRAP v 1.4 (Bell et al., 2012) was used to calculate branch lengths for further phylogenetically informed tests. All statistical tests were conducted using RStudio v 1.1.463 (R Core Team, 2018; RStudio, 2015), and the script, which includes data from Tables 1 and 2, is available in S1. A general linear model was used to test the data for violation of common assumption, including normality, nonconstant error variances (heteroscedasticity), multicollinearity, and outliers, and to test for significant correlations between canal cross-sectional areas and head volume (Table 3). The data were log-transformed to ensure normality prior to all further statistical analyses. The data were tested for phylogenetic signal with the R package APE v 5.2 (Paradis et al., 2004) to evaluate the effects of shared ancestry on canal cross-sectional area and head volume and the necessity for phylogenetically informed tests (Table 4). The parameter λ (Pagel's lambda; Pagel, 1999) was calculated and can range from 0, which indicates no phylogenetic signal and that traits evolved independent of phylogeny, to 1, which indicates that there is phylogenetic signal and that variation in the data can be explained by phylogenetic relatedness. The parameter K (Blomberg's K; Blomberg et al., 2003) was also calculated and ranged from 0 to ∞, where values close to 1 indicate that the model fits a Brownian motion model of evolution. Values greater than 1 indicate more divergence than that expected by Brownian motion and values less than 1 indicate more similarity than that expected by Brownian motion.

Common statistical methods used when analyzing datasets that include measures of body size are a generalized least squares regression (GLS) and principal components analysis (PCA) (Brooke et al., 1999; Schulte-Hostedde et al., 2005; Berner, 2011; Symonds and Elgar, 2013). GLS has been used to control for the influence of size by regressing variable Y on some measure of size and using the residuals in further analyses, or by using size as an additional predictor variable and allowing the trait influenced by size to covary. A pGLS was used here to regress canal cross-sectional areas against head volume using the R package nlme 3.1–137 (Pinheiro et al., 2013). The residuals were then used in a pPCA as data that control for the influence of head volume (Graham, 2003).

Prior to data analysis, tests for common assumption violations (e.g., normality, nonconstant error variances, outliers, etc.), including a variance inflation factor test, was conducted to test for multicollinearity (Table 5). Multicollinearity occurs when multiple variables include similar information (linearly correlated) and leads to incorrect model parameterization, decreased statistical power, and limits the ability to determine the relationships between variables (Graham, 2003). The first statistical method deployed was a PLS regression using the R package PLS v2.7-0 (Mevick et al., 2007). A PLS regression is robust to multicollinearity (Wold, 1984) and has similar variable compression properties as a PCA (Haenlein and Kaplan, 2004; Rosipal and Krämer, 2006). The PLS was not phylogenetically informed, but was

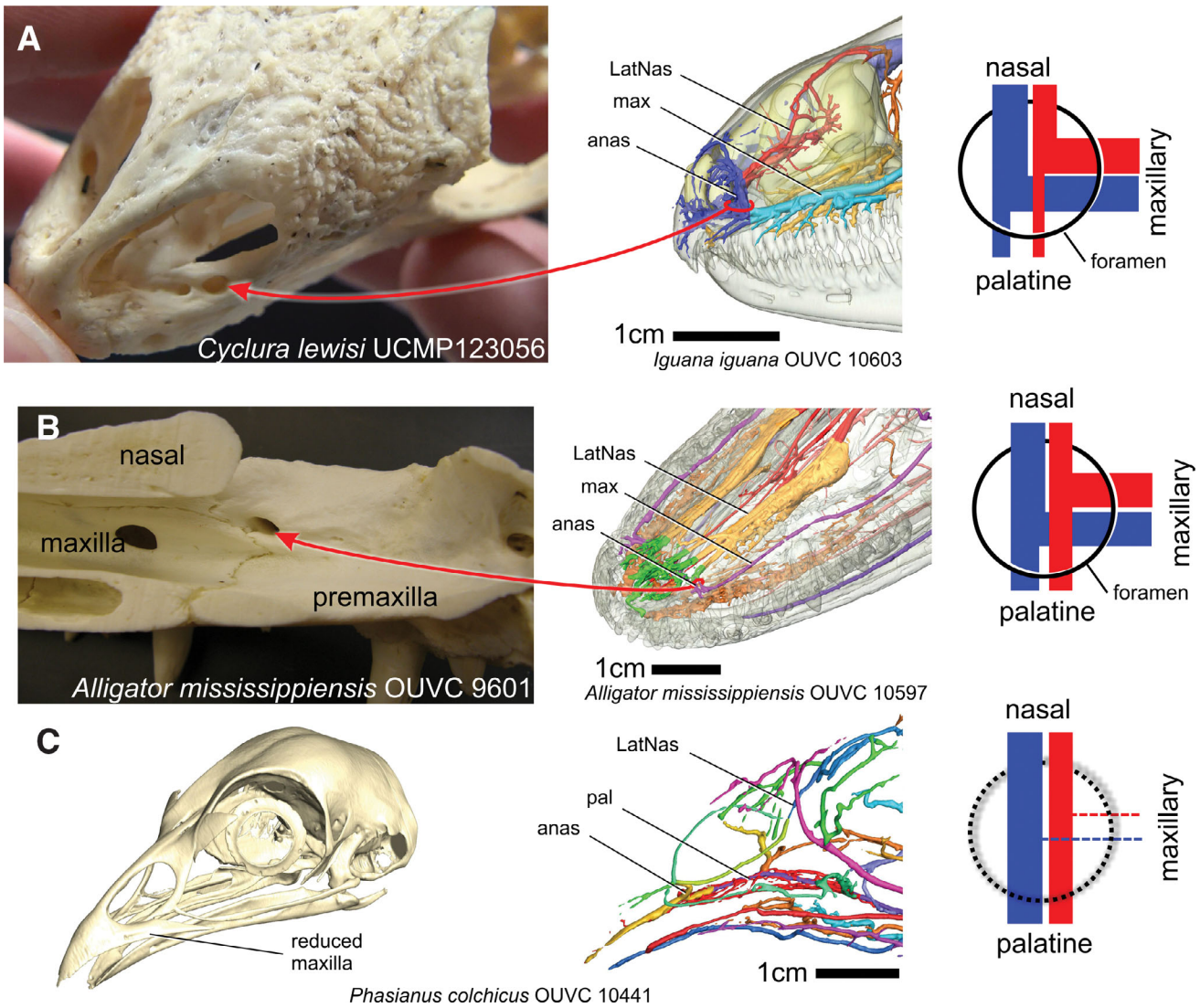

Fig. 4. Vascular osteological correlates found within the narial region of three extant specimens. (**A**) dorsal view of the bony naris in the blue iguana lizard *Cyclura lewisi* (UCMP 123056), (**B**) medial view of the bony naris in *Alligator mississippiensis* (OUVC 10792), and (**C**) oblique view of the ring-necked pheasant *Phasianus colchicus* (OUVC 10441). The blood vessels forming these osteological correlates are the palatine, nasal, and maxillary vessels (middle column). Each blood vessel can contribute more or less blood as the other blood vessels, measured by blood vessel size (right column). Extant taxa demonstrate roughly equal contributions, represented by the size of the red and blue bars, to the anastomosis. The circle represents the bony foramen the vessels pass through (osteological correlate). Abbreviations: anas, anastomosis; LatNas, lateral nasal vessels; max, maxillary vessels; pal, palatine vessels.

specifically used as a multicollinearity robust test that could probe the data for effects that head volume and body mass have on canal cross-sectional area, and for interactions between head volume and body mass.

Like the PLS, a PCA simultaneously examines the multivariate dataset and compresses variables into linearly uncorrelated variables and tests for components that explain the most variance (Peres-Neto et al., 2003). A pPCA was conducted using the R package PHYTOOLS v0.6-60 (Revell, 2012). The pPCA was used on residuals collected from a pGLS regression to specifically control for the influence of head volume on canal size. This method was used to estimate the effect of head volume on canal size, and any signal detected thus would reflect blood flow required to support head tissues. Results from this test were interpreted to be independent of blood flow supporting the basic nutritional needs of the tissues, and observed canal size was in response to other pressures, specifically as part of a thermoregulatory strategy.

Significant pPCA axes (Table 7) were found using the broken-stick method that iteratively and randomly averages the eigenvalues of each axis (Jackson, 1993). An axis was considered significant if the amount of variance explained by each axis was larger than the broken-stick variance (Jackson, 1993). Significant variable loadings for each axis were found using the Guttman-Kaiser Criterion (Yeomans, 1982). This criterion measures the average variance explained by each response variable, and

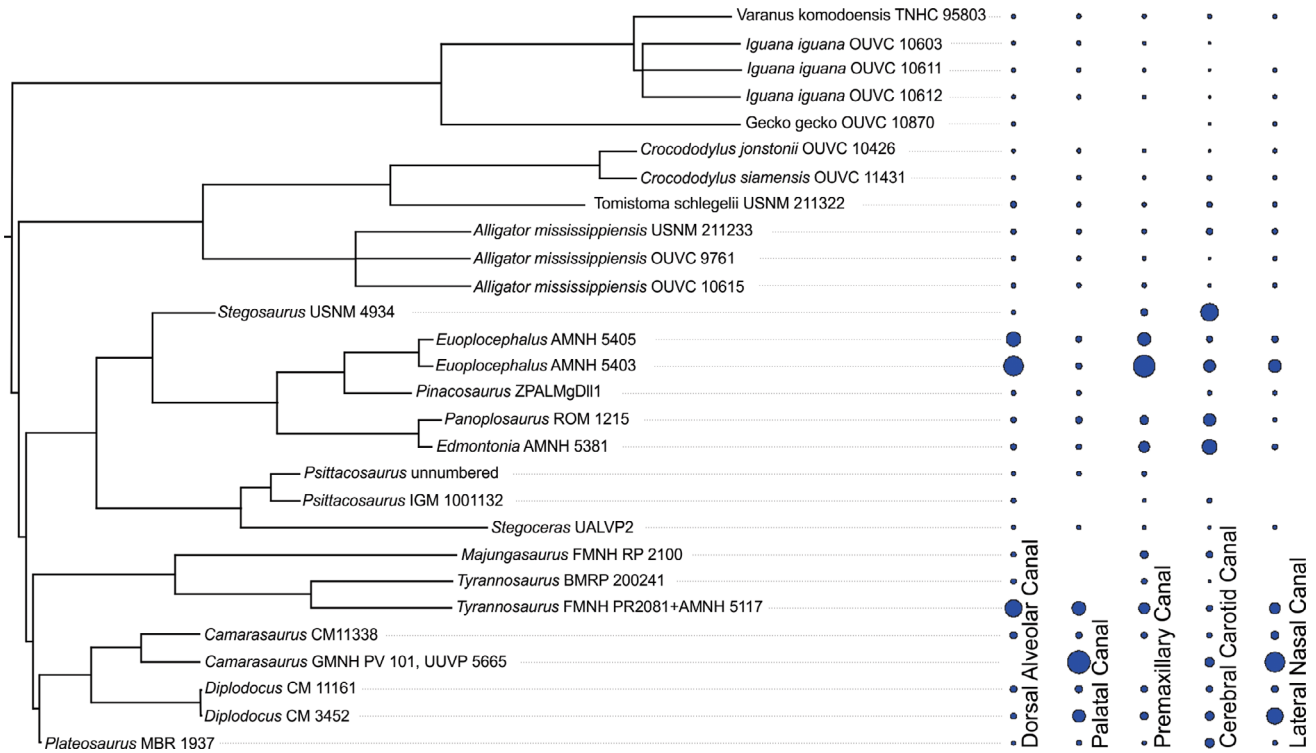

Fig. 5. Phylogeny of sampled diapsids showing topology and branch lengths calculated from occurrence ranges. Topologies modified from Butler et al. (2008), Hocknull et al. (2009), Heinicke et al. (2012), Thompson et al. (2012), Royo-Torres (2014), and Watanabe and Slice (2014). Occurrence ranges were modified for taxa with overlapping temporal ranges by randomly assigning 100,000 years to ensure a fully dichotomous tree. The relative size of each neurovascular canal measured is shown on the right.

loadings that are larger than this value are considered significant (Yeomans, 1982).

Although common in paleontological datasets, missing data is not allowed in many statistical tests, and pPCA and PLS are no exceptions. Missing data reduced the number of taxa in the data set to 19 taxa (two iguanas, one large *Varanus*, six crocodilians, and ten dinosaur taxa). To address missing data due to the incomplete preservation of skulls, multiple specimens of *Camarasaurus* and *Tyrannosaurus* were used to create single composite specimens of each species. Specifically, the braincase of UMNH VP 5665 was paired with the skull of GMNH PV 101, and the braincase of AMNH 5117 was paired with the skull of FMNH PR 2081 to create more complete specimens of *Camarasaurus* and *Tyrannosaurus*, respectively.

INSTITUTIONAL ABBREVIATIONS

AMNH, American Museum of Natural History, New York City, New York; **BMR**, Burpee Museum of Natural History, Rockford, Illinois; **CM**, Carnegie Museum of Natural History; **CMNH**, Cleveland Museum of Natural History, Cleveland, Ohio; **FMNH**, Field Museum of Natural History, Chicago, Illinois; **MB.R.**, Collection of Fossil Reptilia, Museum für Naturkunde, Berlin, Germany; **MNN**, Musée National du Niger, Niamey, Niger; **MOR**, Museum of the Rockies, Bozeman, Montana; **MPC**, Mongolian Paleontological Center, Ulaanbaatar, Mongolia; **THNC**, University of Texas Natural History Collections; **ROM**, Royal Ontario Museum, Toronto, Ontario; **UCPC**, University of Chicago Paleontological Collection, Chicago, Illinois; **UUMNH**, University of Utah Museum of Natural History, Salt Lake City, Utah; **YPM**, Yale Peabody Museum of Natural History, New Haven, Connecticut; **UALVP**, University of Alberta Laboratory for Vertebrate Paleontology, Edmonton, Alberta, Canada; **UCMP**, University of California Museum of Natural History, Berkeley, California; **USNM**, United States National Museum of Natural History, Smithsonian Institution, Washington D.C.; **ZPAL**, Institute of Paleobiology, Polish Academy of Sciences, Warsaw, Poland.

RESULTS

A qualitative anatomical analysis was conducted to compare morphological data from fossils, CT scans, and gross dissections of extant taxa. A quantitative statistical analysis is present immediately thereafter.

Anatomical Analysis

Neurovascular canals. Neurovascular bundles—arteries, veins, and nerves—traveled through most of the canals investigated here. As noted above, determining the relative proportions of the contents of these canals (i.e., neural vs. arterial vs. venous, or their relative contributions) is a critical task for this study and was a major focus of the extant studies (Porter and Witmer, 2015, 2016; Porter et al., 2016). In some cases, these relationships are clear. For example, an exclusively vascular osteological

TABLE 2. List of occurrence ranges used to calculate branch lengths for phylogenetically informed statistical tests

Taxon	Abbreviation	First occurrence date (ya)	Last occurrence date (ya)	Reference
Alligator mississippiensis OUVC 9761	Alli-9761	47,250,000	1	Oaks (2011)
Alligator mississippiensis OUVC 10615	Alli-10615	47,250,000	1	Oaks (2011)
Alligator mississippiensis USNM 211233	Alli-21233	47,250,000	1	Oaks (2011)
Camarasaurus CM 11338	Cama-11338	163,000,000	145,000,000	Woodruff and Foster (2017)
Camarasaurus GMNH PV 101 + UMNH VP 5665		163,000,000	145,000,000	Woodruff and Foster (2017)
Crocodylus johnstoni OUVC 10426	Croc-10426	10,600,000	1	Oaks (2011)
Crocodylus siamensis OUVC 11431	Croc-11431	5,950,000	1	Oaks (2011)
Diplodocus CM 3452	Diplo-3452	157,000,000	145,000,000	Tschopp et al. (2015)
Diplodocus CM 11161	Diplo-11161	157,000,000	145,000,000	Tschopp et al. (2015)
Edmontonia AMNH 5381	Edmo-5381	77,000,000	76,000,000	Arbour et al. (2009)
Euoplocephalus AMNH 5403	Euop-5403	77,000,000	76,000,000	Arbour and Currie (2013); Penkalski (2014)
Euoplocephalus AMNH 5405	Euop-5405	77,000,000	76,000,000	Arbour and Currie (2013), Penkalski (2014)
Gekko gecko OUVC 10870		10,000,000	1	Heinicke et al. (2012)
Iguana iguana OUVC 10603		8,900,000	1	Malone et al. (2017)
Iguana iguana OUVC 10611	Igua-10611	8,900,000	1	Malone et al. (2017)
Iguana iguana OUVC 10612	Igua-10612	8,900,000	1	Malone et al. (2017)
Majungasaurus FMNH PR 2100		72,000,000	66,000,000	Krause et al. (2007)
Panoplosaurus ROM 1215	Pano-1215	76,000,000	75,000,000	Arbour et al. (2009), Arbour and Currie (2013)
Pinacosaurus ZPAL MgD-II/1		86,300,000	83,600,000	Hill (2003)
Plateosaurus MB.R.1937	Plat-1937	218,000,000	208,000,000	Prieto-Márquez and Norell (2011)
Psittacosaurus MPC-D unnumbered		125,000,000	121,000,000	Hedrick et al. (2014)
Psittacosaurus IGM 100/1132		125,000,000	121,000,000	Hedrick et al. (2014)
Stegoceras UALVP 2	Steg-2	77,000,000	76,000,000	Sullivan (2003)
Stegosaurus USNM 4934		157,000,000	145,000,000	Galton (2010)
Tomistoma USNM 211322	Tomi-21322	23,230,000	1	Oaks (2011)
Tyrannosaurus rex BMR P2002.4.1		72,000,000	66,000,000	Brochu (2003)
Tyrannosaurus rex FMNH PR 2081 + AMNH 5117	Tyra-2081	72,000,000	66,000,000	Brochu (2003)
Varanus komodoensis TNHC 95803	Vara-95803	3,800,000	1	Hocknull et al. (2009)

Geologic ages were converted into years using Gradstein and Ogg (2004) and Fowler (2017).

correlate located within the narial fossa was the subnarial foramen of crocodilians and iguanid lizards. Gross dissections revealed that only blood vessels passed through the foramen (Porter and Witmer, 2015; Porter et al., 2016). Saurischian dinosaurs had a similar osteological correlate, which is also hypothesized to only contain blood vessels (Porter, 2015). Likewise, only vascular components (the palatine artery and vein) traverse the suborbital fenestra in extant diapsids, and there is no evidence from the fossil record of extinct dinosaurs to indicate that they were any different in this regard. In other cases, the canal or foramen is known to house all three neurovascular components, but one component clearly predominates. For example, in extant archosaurs, the cerebral carotid canal houses the cerebral carotid artery, which is by far the largest constituent of the canal, but the canal also transmits the much smaller cerebral carotid vein. Small nerves are also conveyed along with the blood vessels, specifically, the palatine (parasympathetic) branch of the facial nerve and sympathetic nerves, but these are volumetrically negligible components (Oelrich, 1956; Baumel, 1975; Bubień-Waluszewska, 1979; Sedlmayr, 2002).

A more complex example is the dorsal alveolar canal which transmits the maxillary neurovascular bundle. The

TABLE 3. Results of general linear models regressing log-transformed canal cross-sectional area against log-transformed head volume or body mass

Canal	$F_{(df)}$	P-value	Adjusted R^2
Cerebral carotid	$36.81_{(1,24)}$ | $36.18_{(1,24)}$	<0.001 | < 0.001	0.58 | 0.58
Palatal	$46.05_{(1,21)}$ | $193.1_{(1,20)}$	<0.001 | < 0.001	0.67 | 0.90
Lateral nasal	$55.60_{(1,20)}$ | $171_{(1,19)}$	<0.001 | < 0.001	0.72 | 0.89
Premaxillary	$43.65_{(1,23)}$ | $93.04_{(1,24)}$	<0.001 | < 0.001	0.64 | 0.79
Dorsal alveolar	$85.45_{(1,25)}$ | $59.21_{(1,24)}$	<0.001 | < 0.001	0.76 | 0.70
Head volume	– | $71.91_{(1,25)}$	– | < 0.001	– | 0.73
Body mass	$71.91_{(1,25)}$ | –	<0.001 | –	0.73 | –
Multiple regression	$10.61_{(5,13)}$ | $36.23_{(5,13)}$	<0.001 | < 0.001	0.72 | 0.90

A multivariate general linear model was also conducted. Results are provided in a head volume | body mass format.

TABLE 4. Each canal was tested for phylogenetic signal using both Pagel's λ and Blomberg's K

Canal	Pagel's λ	Log likelihood	P-value	Blomberg's K	P-value
Dorsal alveolar	0.96	−47.5	<0.001	0.32	0.03
Palatal	0.71	−47.5	0.001	0.19	0.08
Premaxillary	0.76	−40.6	<0.001	0.27	0.03
Cerebral carotid	0.70	−42.1	0.001	0.30	0.07
Lateral nasal	0.82	−43.2	0.002	0.29	0.07
Head volume	0.69	−54.9	0.001	0.12	0.26
Body mass	0.85	0.58.1	<0.001	0.52	0.004

TABLE 5. Results of correlation tests between each variable

Canal	Dorsal alveolar	Palatal	Premaxillary	Cerebral carotid	Lateral nasal	Head volume	Log dataset VIF	GLS residual VIF test
Dorsal alveolar	1	–	–	–	–	–	8.74	2.80
Palatal	0.82	1	–	–	–	–	9.62	3.74
Premaxillary	0.83	0.92	1	–	–	–	15.03	4.23
Cerebral carotid	**0.71**	0.83	0.81	1	–	–	4.17	2.09
Lateral nasal	0.92	0.93	0.90	0.81	1		10.41	4.00
Head volume	0.88	0.83	0.81	**0.78**	0.86	1	–	–
Body mass	0.84	0.95	0.90	0.89	0.95	0.86	–	–

The cerebral carotid canal has the least amount of correlation with the dorsal alveolar canal and head volume (marked in bold). Blood vessels that participate in the anastomosis supplying the narial region have a high correlation. The Variance Inflation Factor (VIF) test indicates a reduction of a violation of the PCA assumption of no multicollinearity when using the residuals from the GLS regression.

fact that the relative proportions of the canal's constituents vary in extant taxa complicates the analysis of the canal as being exclusively a thermoregulatory structure, as the ratio of nerve to blood vessel is important to consider when determining blood flow. Extant crocodilians have a maxillary nerve that is larger than the blood vessels accompanying it through the dorsal alveolar canal. This emphasis of the neural component is readily understandable due to the feeding strategy of crocodilians, where a vast array of special sensory organs, called dome pressure receptors, surround the oral margin (von Düring, 1973, 1974; von Düring and Miller, 1979; Soares, 2002) and are innervated by the maxillary and mandibular branches of the trigeminal nerve. George and Holliday (2013) showed in crocodilians that there is a significant correlation between the number of axons in the trigeminal nerve and the size of the bony trigeminal fossa, which is a reflection of trigeminal ganglion size and the number of sensory nerve cell bodies housed within the ganglion. Gutiérrez-Ibáñez et al. (2009) likewise showed that in certain avian clades the principal sensory nucleus of the trigeminal nerve was hypertrophied, indicating an increased somatosensory component from the oral margin. These results indicate that any expansion or emphasis of the trigeminal nerve system, as might be expected in species emphasizing tactile sensitivity, should be reflected in the size of the trigeminal ganglion fossa or trigeminal canal from dinosaur endocasts. Published endocasts of the dinosaurs sampled here—*Majungasaurus* (Sampson and Witmer, 2007), *Tyrannosaurus rex* (Witmer and Ridgely, 2009), *Camarasaurus* and *Diplodocus* (Witmer et al., 2008), *Euoplocephalus* and *Panoplosaurus* (Witmer & Ridgely, 2008; Miyashita et al., 2011), *Stegoceras* (Bourke et al., 2014), and *Stegosaurus* (Leahy et al., 2015), as well as unpublished endocasts of most of the rest of the study sample—indicate that, at least qualitatively, there is little evidence of substantial trigeminal nerve expansion in these species. For this

TABLE 6. Summary of the partial least squares regression of canal size versus head volume

	PLS loadings				
	Head volume + body mass		Head volume:body mass		
Canal	COMP1	COMP2	COMP1	COMP2	COMP3
Head volume	0.56	0.91	–	0.63	0.91
Body mass	0.83	−0.54	–	0.80	−0.42
Head volume: body mass	–	–	0.99	−0.13	–
% Variance explained					
Proportion	0.91	0.09	0.99	0.0008	0.0015
Total	0.91	1	0.99	0.99	1

The first PLS was investigating the influence of head volume and body mass. The second PLS was testing the investigating the interaction between head volume and body mass.

study, there is no *a priori* reason to hypothesize that most dinosaur clades—and certainly not the dinosaur species included in this study—had remarkably increased sensation around the oral margin and a hypertrophied trigeminal nerve (Barker et al., 2017). Further support for this assumption can be found in the *T. rex* maxilla UCMP 118742 (Fig. 6), which shows an external neurovascular foramen near the jaw margin with three grooves separated by two ridges, which are most parsimoniously interpreted as being for the artery, vein, and nerve branches from the maxillary vessels and dorsal alveolar nerve, respectively. The sizes of these grooves are roughly equivalent, providing further support for the base assumption of equivalently sized nerves, arteries, and veins within at least the dorsal alveolar canal. There may be interesting exceptions, such as the putatively aquatic theropod *Spinosaurus* (Ibrahim et al., 2014), but this species is not part of the present study. In order to resolve this important issue, a survey of a large number of diapsids is necessary. This study thus represents a "first pass" at this problem in that only three diapsid clades were sampled (iguanid lizards, birds, and crocodilians), and birds and crocodilians, a critical component of the extant phylogenetic bracket for dinosaurs, have such divergent maxillary nerve sizes. Crocodilians have a large dorsal alveolar nerve, and birds generally have reduced maxillary blood vessels (presumably concomitant with loss of teeth and reduction of the maxillary bone itself). The iguanas in the study appeared to have more equivalently sized nerve, arteries, and veins. This study is testing the null hypothesis that dinosaurs plesiomorphically retained a relatively balanced nerve-to-blood vessel ratio within the measured canals, and if a canal is apomorphically hypertrophied, explanations are sought. As documented below, available evidence suggests that, in at least the study taxa, blood vessels were the main driver of changes in canal size.

Cerebral carotid canal. The cerebral carotid artery supplies tissues within the endocranial cavity but is also a major blood supply to the nasal region (Oelrich, 1956; Burda, 1969; Baumel, 1993; Sedlmayr, 2002; Porter and Witmer, 2015, 2016; Porter et al., 2016). An increase in the surface area of the nasal region should hypothetically lead to a proportional increase in the diameter of the cerebral carotid canal, up to the point where it impinges on neural or other tissues. In extant taxa, the cerebral carotid arteries are likely of sufficient size to supply the endocranial cavity and nasal region simultaneously. The upper limit for cerebral carotid canal size in extant archosaurs is likely found in crocodilians, as they modify encephalic blood supply during development (Burda, 1969) and enlarge the caudal cerebral artery so that it can supply more blood to the nasal region, instead of the smaller rostral cerebral artery as is present in birds and squamates (Porter and Witmer, 2015, 2016; Porter et al., 2016).

The largest measured cross-sectional area of the cerebral carotid canal in this study was found to be 0.58 cm^2 in *Stegosaurus* (USNM 4934; Table 1), with *Edmontonia* (AMNH 5381), *Panoplosaurus* (ROM 1215), and *Euoplocephalus* (AMNH 5405) being only slightly smaller. *Camarasaurus* (UMNH VP 5665) had a canal cross section of 0.26 cm^2 and *Tyrannosaurus* (AMNH 5117) had a value of 0.14 cm^2 (Table 1). These findings indicate that dinosaurs with large head volumes and expanded sites of thermal exchange (e.g., *Camarasaurus*) could not have relied on the cerebral carotid vessels to be the major supply to the nasal region and required collateral blood supply from the external carotid artery, whereas those dinosaurs with smaller heads may have relied more on the cerebral carotid route, which is plesiomorphic (Porter and Witmer, 2015, 2016; Porter et al., 2016). In the entire small-headed dinosaur taxa sampled up to and including *Stegosaurus* (USNM 4934), there was a trend of larger carotid canal cross-sectional area. However, the larger nodosaurid ankylosaurs in the sample (*Edmontonia* and *Panoplosaurus*), showed a pattern that seems to reflect an increase in cerebral carotid canal size. The cerebral carotid canals are large in *Edmontonia* and *Panoplosaurus* (0.48 cm^2 and 0.36 cm^2, respectively; Table 1) and had balanced collateral routes of blood supply that were of similar value, indicating that some vascular pathways

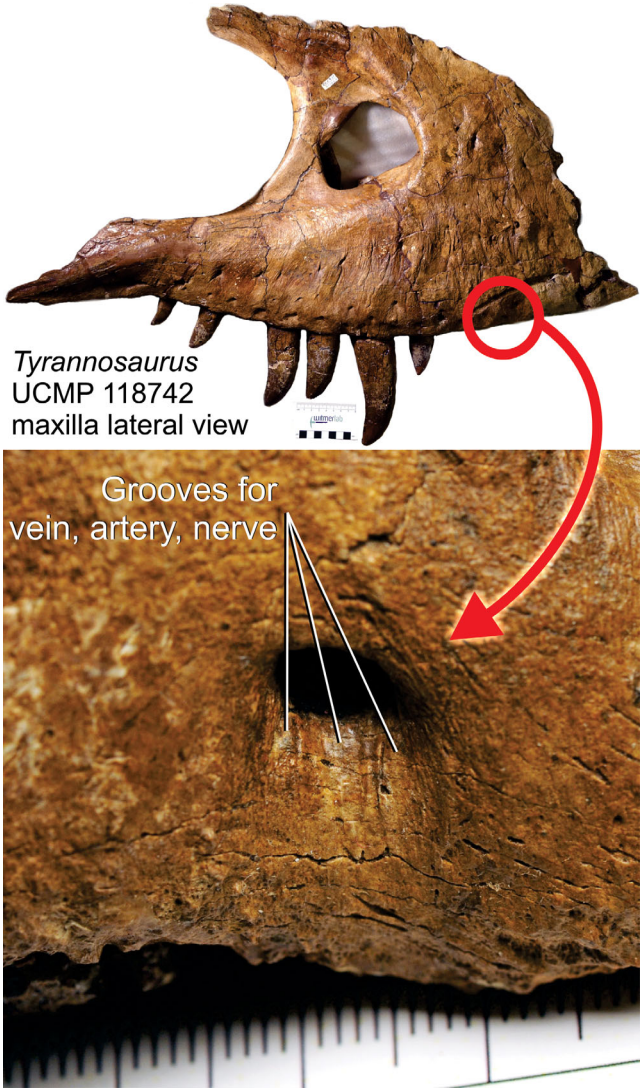

Fig. 6. Lateral view of a *Tyrannosaurus rex* right maxilla (UCMP 118742) showing three grooves emanating from an external neurovascular foramen. These grooves likely indicate the relative sizes of the branches of the dorsal alveolar nerve and maxillary artery and vein supplying the integument at the margin of the bone. The grooves are roughly equivalent in size, providing support for the base assumption of the three components of the neurovascular bundle being similar in caliber.

were not emphasized over others, unlike specimens of their sister-taxon Ankylosauridae (see below). Instead of increasing the size of collateral pathways, blood flow through the endocranial cavity was enlarged in nodosaurids and could have sufficiently supplied the emphasized narial region. This evidence adds support to the hypothesis that the cerebral carotid artery was insufficient in many other dinosaur taxa and that collateral routes of blood supply expanded to compensate.

Dorsal alveolar canal. The dorsal alveolar canal in dinosaurs has received a fair amount of attention in the literature, especially the caudal aspect of the canal as it relates to jaw musculature and paranasal air sinuses (Witmer, 1995, 1997; Holliday and Witmer, 2007). The dinosaurs in this sample had varying dorsal alveolar canal morphologies, from large to nearly undetectable. The rostral portion of the dorsal alveolar canal also shows a variable conformation that may relate to head volume. For example, in smaller-headed dinosaurs, the dorsal alveolar canal exited the maxilla, where it sent blood vessels and nerves along the lateral aspect of the maxilla instead of continuing rostrally through the maxilla or premaxilla. In sauropodomorphs (Fig. 3), this aperture is known as the rostral maxillary foramen (Wilson and Sereno, 1998; Wilson, 2005). In larger-headed dinosaurs, however, the dorsal alveolar vessels continue through the maxilla and premaxilla to exit within the narial fossa in the region of the palatine, nasal, and maxillary vessel anastomosis (Fig. 7B). This finding may indicate that larger-headed dinosaurs either depended on the anastomotic connections to the narial region from the maxillary vessels or that increased bone mass simply captured the vessels such that they traveled through the maxilla and premaxilla; the former option seems more likely but the latter cannot be ruled out.

Sauropodomorpha. Small-headed sauropodomorphs, such as *Plateosaurus* (MB.R.1937; Fig. 3), showed a dorsal alveolar canal morphology similar to that of theropods than of more derived sauropodomorphs. The canal courses dorsal to the tooth row, is straight, and sent multiple branches laterally through the maxilla. The dorsal alveolar canal exits the maxilla caudal to the subnarial foramen as the rostral maxillary foramen.

In larger-headed sauropodomorphs, the dorsal alveolar canal is relatively small (Table 1) and blood provided by it was likely overshadowed by the blood flow through the subnarial foremen. In *Diplodocus* (CM 11161, CM 3452), the maxilla showed no evidence that it contained the maxillary neurovascular bundle within the thin bone (Fig. 8C). One specimen of *Diplodocus* (CM 3452) showed a small canal in the maxilla, just caudal to the preantorbital fenestra, which could have transmitted the entirety of a small neurovascular bundle or just a few small branches of a larger bundle. This osteological correlate was not measured because of the uncertainty of its contents. There is, however, significant evidence that the maxillary neurovascular bundle was present in that numerous grooves are preserved along the rostroventral aspect of the preantorbital fenestra that indicate the presence of neurovascular bundles (Fig. 8A). This finding would indicate that the maxillary neurovascular bundle was indeed present but coursed medial to the maxilla and then ventral to the antorbital sinus. The bundle then curved dorsally along the rostral aspect of the preantorbital fenestra, and then sent multiple neurovascular branches toward the teeth and oral margin (Fig. 8B,D). *Apatosaurus*, *Diplodocus*, and *Nemegtosaurus* show similar evidence for increased vascularization along the rostral portion of the maxilla and premaxilla with grooves coursing rostroventrally from the rostral aspect of the preantorbital fenestra (Berman and McIntosh, 1978; Wilson and Sereno, 1998; Wilson, 2005). The maxillary vessels then curved dorsally along the rostral border of the preantorbital fenestra and reentered the maxilla heading toward the subnarial foramen (Fig. 8C). In CT scans, this canal can be observed connecting the subnarial foramen and the preantorbital fenestra and is interpreted here as the distal end of the dorsal alveolar canal.

Theropoda. Theropods show a consistent dorsal alveolar canal that entered the dorsomedial aspect of the maxilla, ventral to the antorbital sinus. The canal courses rostrally and sends branches toward the teeth and the lateral aspect of the maxilla. The canal opens at the subnarial foramen within the narial fossa (except in *Majungasaurus*), and then continues into the premaxilla to join with the canal for the premaxillary vessels. In juvenile *Tyrannosaurus* (BMR P2002.4.1) and *Majungasaurus* (FMNH PR 2100), which have comparable head volumes (Table 1) the size of the dorsal alveolar canal is comparable to the other canals measured (Table 1), indicating a balanced blood supply. Even in larger specimens of *Tyrannosaurus* (FMNH PR 2081), the dorsal alveolar canal still retains a size similar to that of the other measured canals (Table 1). This finding would indicate that a balanced blood supply to the oral and nasal region occurs in a range of head sizes and is likely a plesiomorphic condition of theropods, although more sampling is need to test this hypothesis further.

Ornithischia. The basal ceratopsian *Psittacosaurus* (MPC-D unnumbered) has a dorsal alveolar canal morphology similar to that of *Plateosaurus* (MB.R.1937). The canal was found dorsal to the tooth row, was straight, and exited the maxilla caudal to the narial fossa. The pachycephalosaurid *Stegoceras* (UALVP 2) has a long and straight dorsal alveolar canal that exited the maxilla within the narial fossa and a groove continued along the dorsal aspect of the premaxilla (Fig. 7C). The largest dorsal alveolar canal in the sample (not just relative to head volume, but absolutely) was found in *Euoplocephalus* (AMNH 5405, 5403), which was also the largest ankylosaur in the sample (2.50 cm^2 and 1.67 cm^2, respectively; Table 1). The palatomaxillary vessels gave off the palatine vessels (which then pass through the small suborbital fenestra) dorsal to the ectopterygoid and then entered the dorsal alveolar canal as the maxillary vessels in the rostroventral aspect of the orbit (Fig. 9; Porter, 2015). The dorsal alveolar canal passed ventral to the rostral loop of the airway (Witmer and Ridgely, 2008), where the roof of the canal was not detectable. This condition is similar to that in iguanid lizards, where there is only a thin membrane roofing the dorsal alveolar canal and separating the maxillary neurovascular bundle from the airway (Oelrich, 1956; Porter and Witmer, 2015). The smallest ankylosaurid in the sample, *Pinacosaurus* (ZPAL MgD-II/1), admittedly a juvenile (Maryańska, 1977), has a dorsal alveolar canal cross-sectional area only slightly larger than all of the other canals measured (Table 1), indicating a relatively balanced blood supply, with a slight bias toward the dorsal alveolar canal.

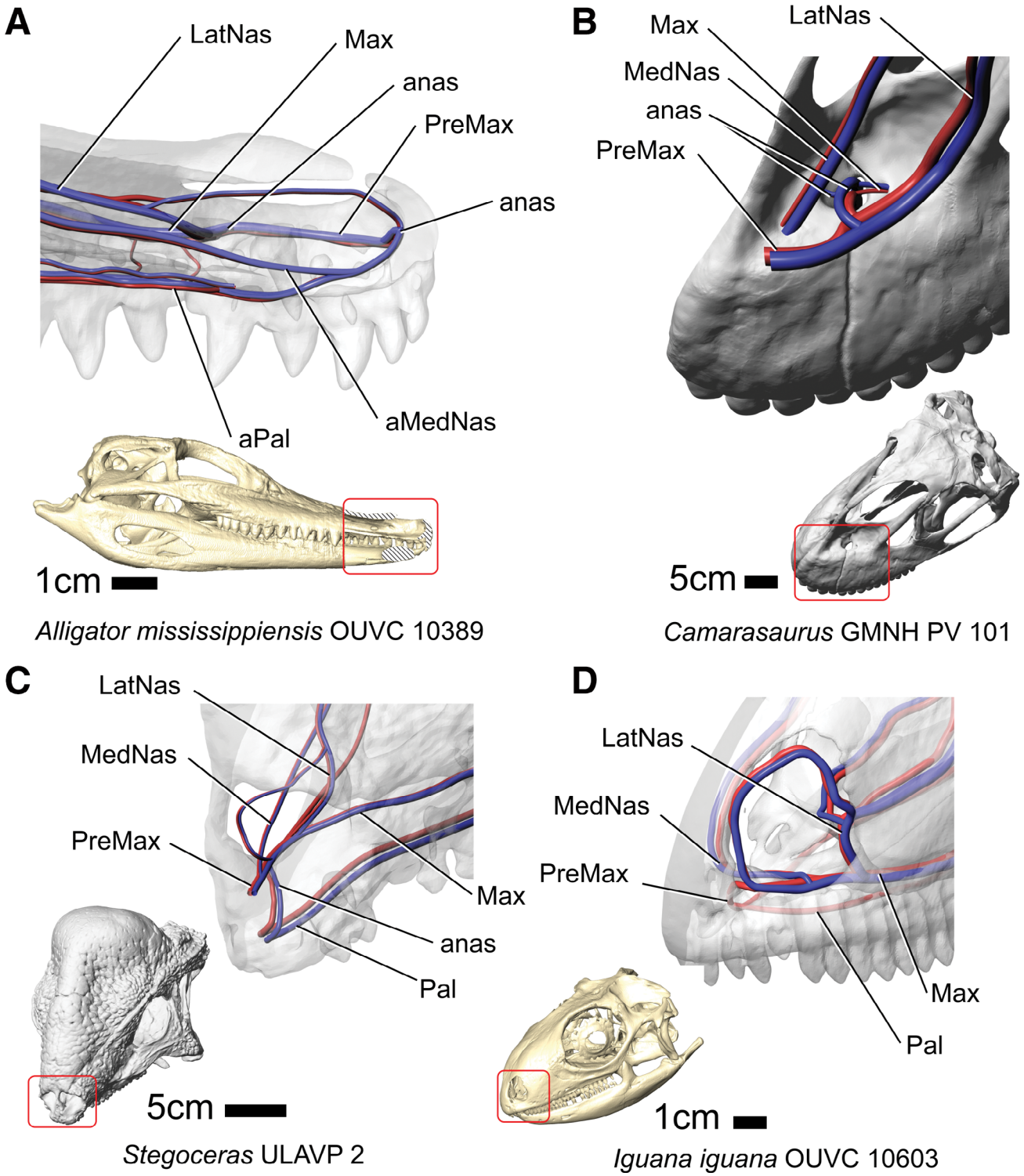

Fig. 7. Narial regions of two extant taxa (**A**) *Alligator mississippiensis* (OUVC 10389) and (**D**) *Iguana iguana* (OUVC 10603) and two dinosaurs (**B**) *Camarasaurus* (GMNH PV 101) and (**C**) *Stegoceras* (UALVP 2) showing blood vessels passing through the narial region and anastomosing. Crocodilians have similar vascular osteological correlates as saurischian dinosaurs, where the palatine vessels anastomose near the maxilla and premaxilla articulation. Iguanid lizards have similar vascular osteological correlates as ornithischian dinosaurs, where the palatine vessels anastomose within the rostral portion of the premaxilla. Abbreviations: anas, anastomosis; LatNas, lateral nasal vessels; Max, maxillary vessels; MedNas, medial nasal vessels, Pal, palatine vessels; PreMax, premaxillary vessels.

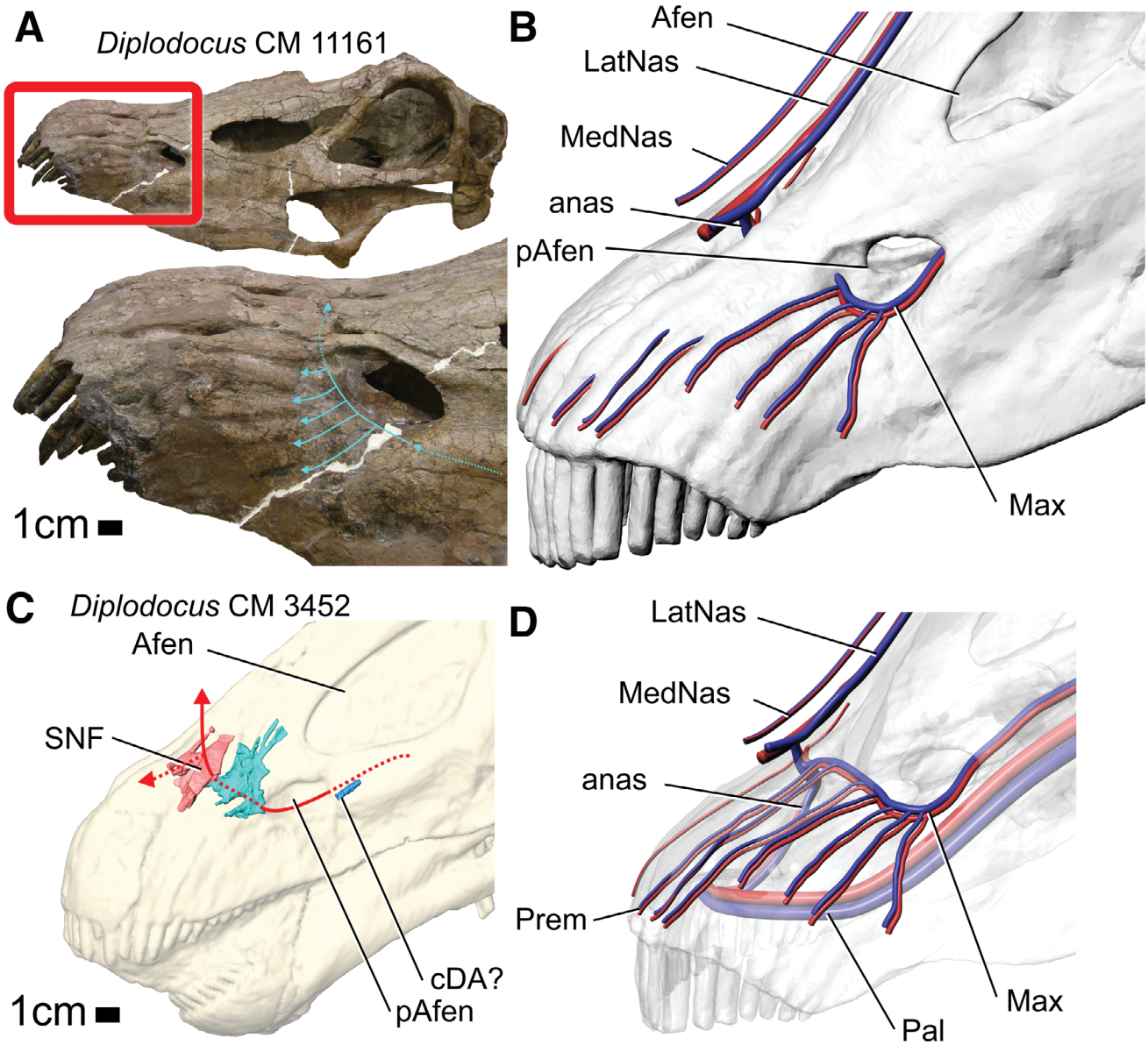

Fig. 8. Lateral views of *Diplodocus* showing (**A**) the fossil (CM 11161) and (**B**) a lateral view showing external blood vessels. (**C**) *Diplodocus* (CM 3452) showing canals associated with the subnarial foramen and dorsal alveolar canal and (**D**) a lateral view with a semitransparent skull to show the internal blood vessels. The maxillary vessels of *Diplodocus* coursed rostrally along the ventral preantorbital fenestra and entered the maxilla to join an anastomosis within the subnarial foramen. Evidence for the maxillary vessels inside the maxilla is inconclusive, with only a small canal to indicate its presence. Abbreviations: anas, anastomosis; LatNas, lateral nasal vessels; Max, maxillary vessels; MedNas, medial nasal vessels; Pal, palatine vessels; PreMax, premaxillary vessels; cDA, dorsal alveolar canal; Afen, antorbital fenestra; pAfen, preantorbital fenestra.

The canal showed a similar course as in the larger *Euoplocephalus*, but lacked clear osteological evidence for the lateral nasal vessels, perhaps in part due to incomplete preservation. In the nodosaurid *Panoplosaurus* (ROM 1215), the dorsal alveolar canal courses dorsal to the tooth row, yet exits the maxilla very early, about halfway to the narial fossa. This pattern is consistent with other dinosaurs with a small head volume. The closely related nodosaurid *Edmontonia* (AMNH 5381), however, showed a vastly different dorsal alveolar canal in that there is no clear canal located dorsal to the tooth row in the maxilla. Along the entire length of the maxilla, two compact layers of bone can be seen with trabeculated bone between them. There is a small and highly branching canal lateral to the maxilla that is associated with the maxillary osteoderm. This canal is interpreted here as the dorsal alveolar canal, as it courses toward the caudoventral aspect of the narial fossa after supplying the osteoderm.

Canal for palatine vessels. Osteological correlates for the palatine vessels do not demonstrate a consistent pattern across both major dinosaur clades. For example, saurischians show evidence for vascular similarities with crocodilians, whereas ornithischians show evidence for

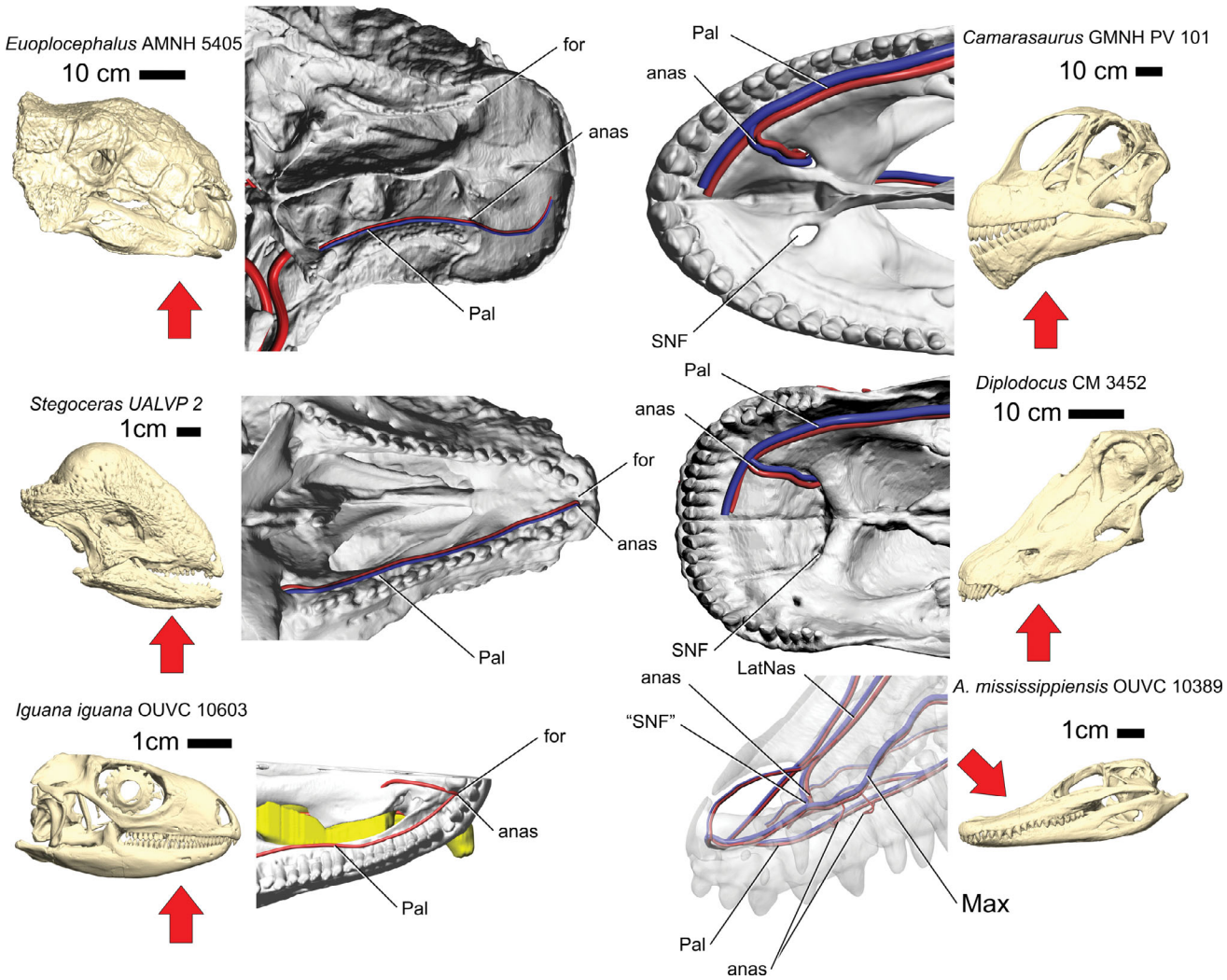

Fig. 9. Ventral view of two extant taxa *Iguana iguana* (OUVC 10603) and *Alligator mississippiensis* (OUVC 10389) (bottom) and four dinosaurs. The differences in the blood supply through the oral region, specifically the palate, can be seen in these dinosaurs. Ornithischian dinosaurs *Euoplocephalus* (AMNH 5405) and *Stegoceras* (UALVP 2), (top two at left) show osteological correlates for small palatine vessels, whereas sauropod dinosaurs, *Camarasaurus* (GMNH PV 101) and *Diplodocus* (CM 11161) (top two at right), show osteological correlates for large palatine vessels. Red arrow indicates the view for the middle images showing restored dinosaur blood vessels. Abbreviations: anas, anastomosis; LatNas, lateral nasal vessels; for, foramen transmitting anastomosis; Max, maxillary vessels; MedNas, medial nasal vessels; Pal, palatine vessels; PreMax, premaxillary vessels; SNF, subnarial foramen.

vascular similarities with iguanid lizards (Figs. 3–4, 6–8). In crocodilians (and saurischians), a canal within the maxilla–premaxilla suture transmits an anastomotic branch between the lateral nasal, palatine, and maxillary vessels (Fig. 9; Porter, 2015; Porter et al., 2016). The ornithischian anastomosis is similar to iguanid lizards, where branches of the nasal and palatine vessels pass dorsally through the rostral aspect of the premaxilla (Fig. 9; Porter, 2015; Porter and Witmer, 2015).

Theropoda. The palatal side of the subnarial foramen was measured as a proxy for the palatine vessels. This foramen is well known in saurischians (Gauthier, 1986) and has been documented in numerous theropods (Weishampel et al., 2004; Porter, 2015). In *Tyrannosaurus* (FMNH PR 2081) the nasal and palatal sides of the subnarial foramen, as well as the dorsal alveolar canal, are very similar in size (Table 1), which suggests balanced blood flow between the oral and nasal region. *Majungasaurus* and other abelisaurids are unusual in not having a subnarial foramen (Sampson et al., 1996; Sampson and Witmer, 2007), but they still show all of the other features of the maxillary neurovascular bundle on the lateral aspect of the maxilla, indicating that a loss of the subnarial foramen had little impact on the maxillary nerve, adding evidence to the hypothesis that the subnarial foramen was an exclusively vascular dinosaurian osteological correlate.

Sauropodomorpha. In *Plateosaurus* (MB.R.1937), the palatal side of the subnarial foramen was found between the maxilla and premaxilla, lateral to the vomer, and slightly dorsal to the longitudinal row of dental

nutrient foramina. The palatal side was found to have a similar diameter as the lateral nasal side of the subnarial foramen (0.22 cm^2 and 0.21 cm^2, respectively; Table 1). *Plateosaurus* was a dinosaur with a modest head volume that had a slightly expanded narial region. The blood supply to this region was starting to show an imbalance, as the dorsal alveolar canal did not match the size of the subnarial foramen. The large cerebral carotid canal of *Plateosaurus* (MB.R.1937) may also indicate that the cerebral carotid vessels were nearing the limit of their ability to supply the narial region.

Sauropods in general have a large subnarial foramen that leads directly between the oral and narial regions (Figs. 7–9). *Diplodocus* has a dorsally located, slit-like subnarial foramen that passed through the maxilla just caudal to the premaxilla (Fig. 8C). The position of the palatal side of the subnarial foramen is medial to the vomerine process of the maxilla in *Diplodocus*, (McIntosh and Berman, 1975; Upchurch, 1999) and *Camarasaurus* (Upchurch, 1999). In *Diplodocus* (CM 11161), the palatal side of the subnarial foramen was similar in size to the lateral nasal canal (Table 1). The size similarity of this canal suggests continuity of blood flow between the oral and nasal regions. All of the sampled sauropods demonstrate a sizeable subnarial foramen and modest dorsal alveolar canal (which likely reflected the size of the plesiomorphic neurovascular bundle within), adding evidence to support the hypothesis that both the oral and narial regions in sauropods were emphasized sites of thermal exchange. *Camarasaurus* (UMNH VP 5665) had the same cerebral carotid canal size as *Plateosaurus* (MB.R.1937; Table 1), which had a head volume 27 times smaller, indicating that the cerebral carotid vessels were not able to supply sufficient blood to the narial region in large sauropods and that collateral circulation from branches of the external carotid artery were recruited.

Ornithischia. The sampled ornithischians showed a variable contribution of the palatine vessels to the maxillary, nasal, and palatine anastomosis. *Psittacosaurus* (MPC-D unnumbered) demonstrated a small canal in the premaxilla that contained the anastomotic branches of the palatine vessels. You et al. (2008) reported the presence of a foramen in *Psittacosaurus* that may have housed dorsally directed branches of the palatine vessels. Canals that housed palatine vessel branches have also been reported in *Maiasaura* (Horner 1983). This same condition was described in *Lesothosaurus* by Sereno (1991), providing further evidence that a wide array of ornithischians housed the palatine anastomotic branches within the premaxilla.

Ankylosaurs demonstrated a similar morphology as the smaller-headed ornithischians. The canal in the premaxilla did show some variation, as *Euoplocephalus* did not have palatine canals completely within the premaxilla, but the foramen was located between the maxilla and premaxilla, similar to theropods (Fig. 9). Other ankylosaurs had the palatine canal within the rostral portion of the premaxilla. These foramina in *Euoplocephalus* were first described by Gilmore (1914) and are known from multiple specimens. Maryańska (1977) reported that the foramina were related to the vomeronasal (Jacobson's) organ, but this hypothesis has been rejected due to the lack of a vomeronasal organ in crown archosaurs (Senter, 2002). The hypothesis that these foramina transmitted anastomotic branches between the palatine and nasal vessels (Witmer, 2001; Hill et al., 2003) is more consistent with the anatomical data.

In *Euoplocephalus* and *Panoplosaurus*, the size of the palatine canal suggests that larger blood vessels were passing between the narial and oral regions. In *Euoplocephalus and Stegoceras*, however, the suborbital fenestra is small, indicating that the palatine vessels that passed through it also were small (Fig. 9), which may indicate that the dorsal alveolar vessels were supplying the rostral palatal area, with little contribution from the palatine vessels, which would have allowed the palatal region to act as another, albeit smaller, site of thermal exchange.

Canal for lateral nasal vessels. Osteological correlates for the lateral nasal vessels were variable and not always present in both extant and extinct taxa. Iguanas demonstrated a foramen along the caudoventral aspect of the narial fossa that transmits an anastomotic connection between the lateral nasal and dorsal alveolar vessels (Fig. 9). Crocodilians demonstrate a similar anastomosis between the lateral nasal and maxillary vessels (Fig. 9).

Ornithischia. The sampled ornithischian dinosaurs did not consistently have osteological correlates for the lateral nasal vessels. *Stegoceras* (UALVP 2) and ankylosaurs did offer some evidence for the lateral nasal vessels due to their prominent hypermineralization (Bourke et al., 2014; Porter, 2015). *Euoplocephalus* (AMNH 5403, 5405) has large nasal canals (Witmer and Ridgely, 2008) that shared a connection with the dorsal alveolar canal in the caudoventral aspect of the narial fossa. The large size of these canals and the small palatal canals suggests that blood flow to the narial region was much larger than blood flow to the oral region. *Edmontonia* (AMNH 5381) has a similar head volume as *Euoplocephalus*, yet demonstrated a plesiomorphically small dorsal alveolar canal, indicating that it likely retained the predominance of cerebral carotid artery supply to the nasal region. *Pinacosaurus* (again, a juvenile specimen), *Edmontonia*, and *Panoplosaurus* did show evidence for an emphasis or enlargement of the narial region (Witmer and Ridgely, 2008), yet the lateral nasal and dorsal alveolar canals had a more balanced vascularization, indicating a sufficient carotid blood supply.

Euoplocephalus had a large canal caudal to the premaxillary canal that contained the medial nasal vessels. Ankylosaurs, which are now well known for long and convoluted airways (Witmer and Ridgely 2008; Miyashita et al., 2011), possess evidence for both the medial and lateral nasal vessels. These large canals are likely too large to be mainly arterial (given that in potentially all amniotes a large majority of the total blood volume at any one time is on the venous side). This may indicate that veins were also a large component of the medial nasal canals, which is consistent with the hypothesis that the narial region was expanded for a significant thermoregulatory role that would influence temperatures of neurosensory tissues in that these veins could have drained to the endocranial cavity (Porter, 2015; Porter and Witmer, 2015, 2016; Porter et al., 2016).

Sauropodomorpha. The location of the subnarial foramen was slightly different between *Plateosaurus*, *Diplodocus*, and *Camarasaurus*. The subnarial foramen is still anatomically located between the maxilla and premaxilla, but is positioned to face dorsally in *Camarasaurus* and *Diplodocus* (Upchurch, 1999), and laterally in *Plateosaurus*

(Wilson and Sereno, 1998; Upchurch, 1999; Prieto-Márquez and Norell, 2011), which is similar to theropods and is the plesiomorphic condition (Gauthier, 1986). *Camarasaurus* (CM 11338, also a juvenile specimen) and *Diplodocus* (CM 3452, CM 11161) had a large lateral nasal side of the subnarial foramen (Figs. 7–9). *Euoplocephalus* and *Camarasaurus* show convergently expanded narial regions with evidence for enhanced blood flow. When compared to ankylosaurs, sauropods show evidence for enhanced blood flow between the oral to the narial regions, where ankylosaurs seem to largely exclude the oral region.

Theropoda. *Tyrannosaurus* (FMNH PR 2081) demonstrated a relatively balanced cross-sectional area between the lateral nasal, palatine, and dorsal alveolar canals. *Majungasaurus* and a juvenile *Tyrannosaurus* specimen (BMR P2002.4.1) also had canals of similar size and appeared balanced like the larger theropod specimen. Because of this balanced vascularization, theropods likely did not particularly emphasize one of the traditional sites of thermal exchange over the others. The nasal and oral regions of the head were generally of the same relative size as much smaller theropods. Unfortunately, *Tyrannosaurus* (FMNH PR 2081) was the only theropod in the sample that clearly demonstrated all of these canals, so generalizable conclusions that relate to this broad pattern are limited.

Antorbital air sinus. The antorbital air sinus of extant archosaurs (Witmer, 1997) is a well-vascularized structure (Sedlmayr, 2002). Branches from the maxillary vessels supply and drain the sinus, which usually demonstrates a fine, highly branched configuration. In birds, the paranasal sinus system is actively ventilated, as diverticula weave between the jaw muscles, forcing air in and out of the paranasal sinuses like a bellows pump (Witmer, 1995, 1997; Witmer and Ridgely, 2008). Crocodilians do not actively ventilate the paranasal sinuses (Witmer, 1995, 1997).

The expanded paranasal sinus system of theropods had the potential to be an emphasized site of thermal exchange if indeed the sinuses were both actively ventilated (as seems likely; Witmer, 1997; Witmer and Ridgely, 2008) and well vascularized. Evidence for the blood vessels vascularizing the antorbital sinus in extinct dinosaurs has not been well described previously but is apparent in many specimens (Fig. 9). Sampson and Witmer (2007, see also Delcourt, 2018) indicated that much of the rugose texture of the facial bones in the abelisaurid theropod *Majungasaurus* was caused by metaplastic ossification of the dermis that surrounded blood vessels, leaving detectable grooves, canals, and foramina in the craniofacial bones, especially those surrounding the antorbital fossa. Sereno et al. (2004) reported grooves along the entire lateral surface of the maxilla ventral to the antorbital fossa in the abelisaurid *Rugops* (Fig. 11A). The maxillary grooves usually continue their course from the surface of the maxilla dorsally across the ventral margin of the antorbital fossa. The dorsal ends of these grooves are open, which we interpret as suggesting that in life the vessels running in these grooves would have passed laterally over the surface of the antorbital sinus. Very similar grooves are found in *Majungasaurus* (Fig. 10). These grooves typically connect with foramina in the maxilla found ventral to the antorbital fossa (Fig. 10C), indicating that branches from the maxillary vessels exited the lateral surface of the maxilla, turned dorsally along the maxilla and continued dorsally to supply the ventral aspect of the antorbital sinus. Most of these grooves course along the surface of the maxilla and right off of the dorsal edge of the bone, indicating there were continuous blood vessels passing from the maxilla to the antorbital sinus. An additional groove was found on the ventral aspect of the antorbital fossa in *Rugops* (Sereno, 2004) and *Majungasaurus*, indicating a separate branch from the maxillary vessels traveled between the maxilla and the ventral edge of the antorbital sinus that likely anastomosed with the blood vessels exiting the maxilla and traveling to the antorbital sinus. It is worth noting here that although there certainly were trigeminal nerve branches running with some of these vessels, the highly anastomosing character of the grooves is more consistent with vasculature, confirming that blood vessels were probably more important players in shaping this morphology.

Evidence in other nonavian theropods similar to that found in the ceratosaurian abelisaurids *Rugops* and *Majungasaurus* indicates that having blood vessels associated with the antorbital sinus probably characterizes other theropod clades as well. For example, along the large ridge of the ventral antorbital fossa on the maxilla of the tetanuran allosauroid *Carcharodontosaurus* (SGM DIN 1), robust grooves course along the ventrolateral aspect of the ridge without exiting through maxillary foramina (Fig. 11B). As in the abelisaurids, these blood vessels are likely covering the rostroventrolateral aspect of the antorbital sinus, providing evidence for the amount of vascularization of the sinus. Likewise, the maxilla of *Allosaurus* (UMNH VP 18047) has a series of foramina ventral to the interfenestral strut (Witmer, 1997) that have a direct connection to the dorsal alveolar canal, which demonstrates that the maxillary vessels were supplying this region, as in extant archosaurs. Among coelurosaurs, in *Tyrannosaurus* (e.g., CM 9380, BMR P2002.4.1), the row of foramina exiting the lateral surface of the maxilla shows dorsally directed grooves that likely anastomosed with the blood vessels coming from the antorbital sinus. The blood vessels supplying the ventral aspect of the antorbital sinus likely branched off of the maxillary vessels before they entered the dorsal alveolar canal, which would be consistent with evidence for an otherwise balanced pattern of blood flow in theropods.

Other bones that comprise the border of the antorbital cavity shows evidence for blood vessels associated with the antorbital sinus. The lacrimal bones of *Albertosaurus* (AMNH 5336), *Daspletosaurus* (FMNH PR 308), *Tyrannosaurus* (FMNH PR 2081; BMR P2002.4.1; CM 9380), *Majungasaurus* (FMNH PR 2100), and *Rugops* (MNN IGU1) show rostrally directed grooves on the lateral surface that are associated with the antorbital sinus (Figs. 9 and 10). These blood vessels would have anastomosed with vessels from the orbital region, as grooves on the orbital surface of the lacrimal (Figs. 10B and 11C) lead to foramina that exit on the lateral surface of the bone (Fig. 11D,E). Additional grooves for blood vessels anastomosing with orbital vasculature were found along the dorsolateral surface of the lacrimal. These grooves course along the dorsolateral surface of the lacrimal, send branches to the dorsal aspect of the skull, or continue rostrally to the antorbital sinus (Fig. 11D). The medial surface of a *T. rex* lacrimal (Fig. 11C) shows these grooves in fine detail and shows that the orbital vasculature anastomosed with the antorbital sinus vasculature (Fig. 11E).

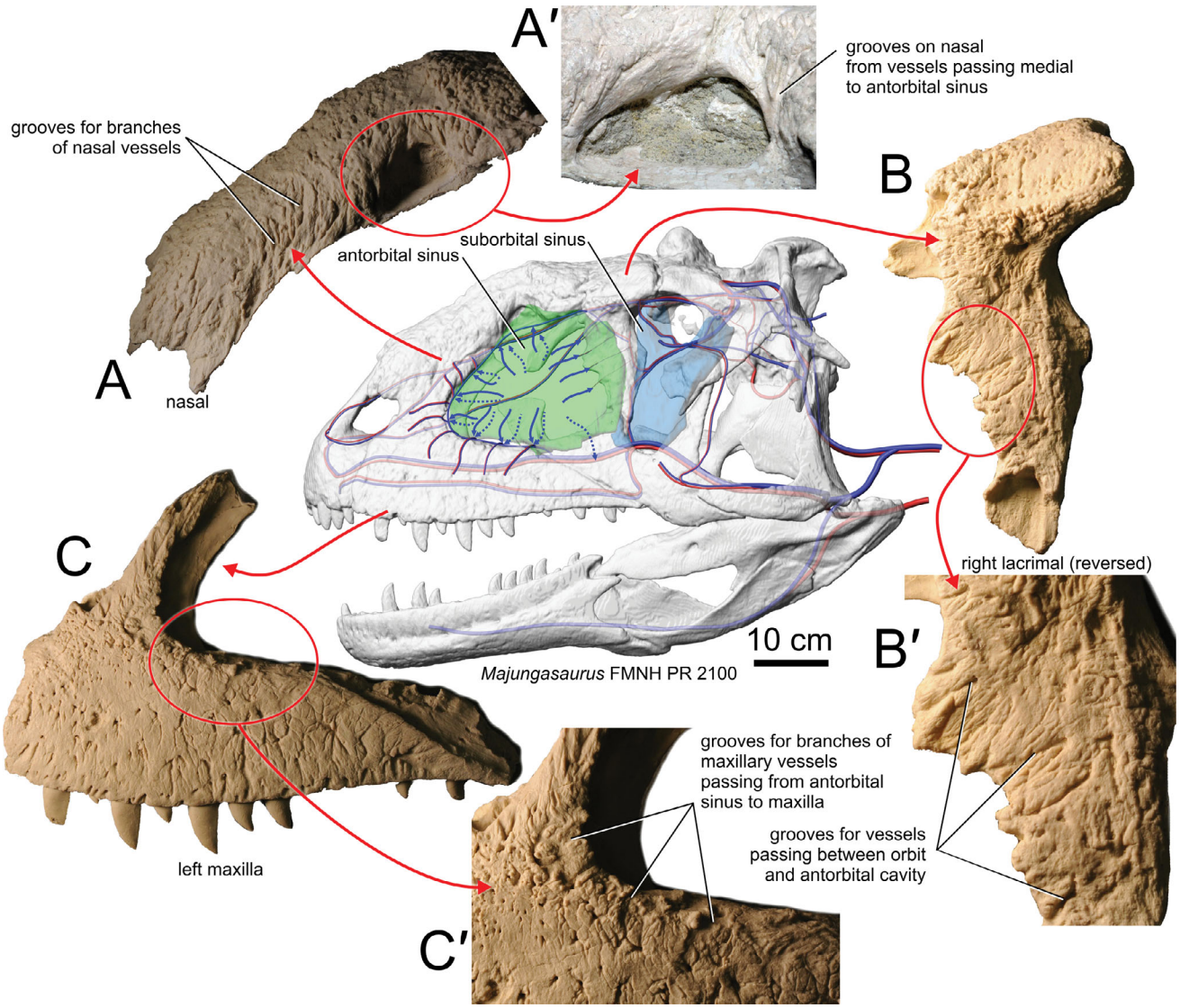

Fig. 10. *Majungasaurus* (FMNH PR 2100) in left lateral view showing evidence for vascularization of the antorbital air sinus on the bones surrounding the antorbital cavity. The antorbital paranasal air sinus (green) is shown covered with blood vessels (blue lines) that originate from and drain to the maxillary, nasal, and orbital vessels. (**A**) *Majungasaurus* nasal bone (cast) in left lateral view showing grooves that housed blood vessels passing between the nasal vessels to the antorbital sinus. (A′) close-up of *Majungasaurus* nasal bone (actual fossil) showing grooves for blood vessels passing along the nasal from the medial surface of the antorbital sinus. (**B**) *Majungasaurus* right lacrimal bone (cast; reversed) in right lateral view. (B′) close-up of *Majungasaurus* right lacrimal (cast; reversed) showing grooves and foramina that indicate blood vessels passing through and lateral to the lacrimal bone between the orbit and the antorbital sinus. (**C**) *Majungasaurus* left maxilla (cast) in left lateral view. (C′) close-up of *Majungasaurus* left maxilla (cast) showing grooves for blood vessels passing along the lateral aspect of the maxilla, often from foramina that lead to the maxillary vessels, that course dorsally. The groove ends along the edge of the maxilla, indicating that the blood vessels are traveling between the maxilla and the lateral surface of the antorbital sinus.

The same dinosaurs indicated above show grooves on the dorsal and lateral aspects of the nasal bones that indicate that the nasal vessels could also been involved with supplying the antorbital sinus (Fig. 11A). Grooves for blood vessels can be seen along the ventrolateral aspect of the nasal bordering the dorsal portion of the antorbital sinus, coursing from what would have been both the medial and lateral aspects of the sinus to grooves that would have led to anastomotic connections with the lateral nasal vessels. This pathway would provide a direct link to veins that would deliver cooled blood to the nasal vessels and then into either the dural venous sinuses or the orbital vasculature.

Even dinosaurs without emphasized antorbital sinuses, such as *Brachiosaurus* (USNM 5730) offer evidence for the vascularization of the antorbital sinus. Within the depression on the medial side of the maxilla, dorsal to the supralveolar lamina (Witmer, 1997) and palatine process of the maxilla, there are distinct, bifurcating vascular grooves. The blood vessels creating these grooves were likely branches of the maxillary vessels that coursed along the dorsal aspect of the maxilla and ventral to the

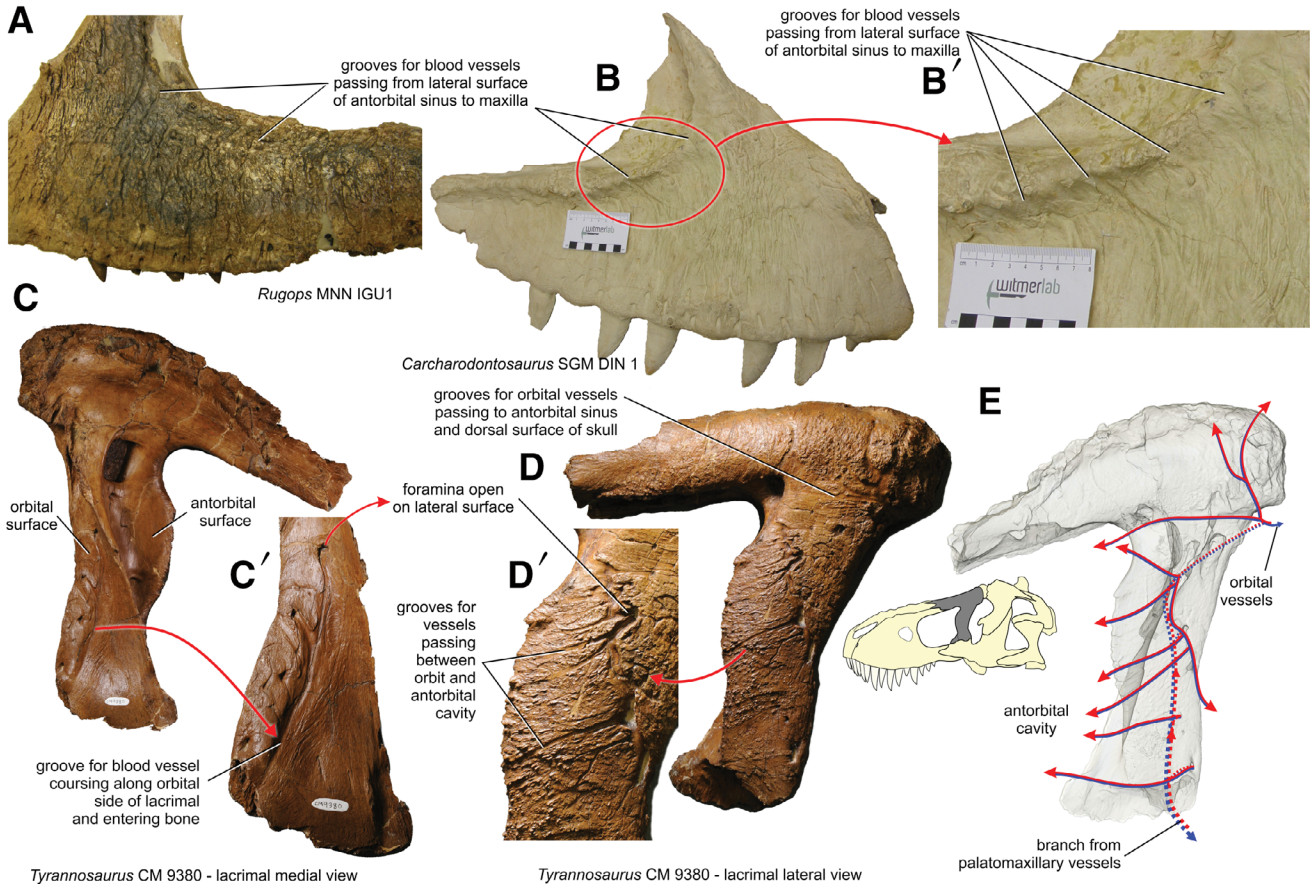

Fig. 11. Evidence for enhanced vascularity of the antorbital paranasal air sinus in nonavian theropods. (**A**) Left maxilla of the ceratosaurian abelisaurid theropod *Rugops* (MNN IGU 1) in lateral view. Vascular grooves associated with the air sinus can be found on the lateral aspect of the maxilla. (**B**) Right maxilla of the allosauroid carcharodontosaurid theropod *Carcharodontosaurus* (SGM DIN 1) in lateral view. (B′) Enlargement of (B) showing large grooves on the maxilla that pass from the antorbital sinus onto the maxilla. There are no foramina along the edge of the ridge demarcating the antorbital fossa that the blood vessels passing from the maxillary vessels to the lateral surface of the maxilla could have originated from. (**C–E**) Left lacrimal of *Tyrannosaurus rex* (CM 9380); inset of full skull shows the position of the lacrimal in the skull (modified from Hurum and Sabat, 2003). (C) Medial view showing a large vascular groove on the orbital surface. (C′) Close-up of the groove shown in (C). This groove indicates that the palatomaxillary blood vessels in the ventral orbital region passed along the lacrimal, entering foramina that open onto the lateral surface of the lacrimal [shown in (D′)]. (D) Lateral view showing large grooves for blood vessels supplying the antorbital sinus. (D′) Close-up of the groove in (D) for branches of the palatomaxillary vessels passing to the antorbital sinus. Additional grooves passing from the rostrodorsal aspect of the orbit along the lateral aspect of the lacrimal were also found. The supraorbital vessels, or the anastomotic connection between the infraorbital and palatomaxillary vessels, likely supplied the blood vessels making these grooves. (E) Left lateral oblique view of CT-scan data rendered semitransparent, showing a diagram of the blood vessels passing along the medial and lateral surfaces of the lacrimal.

sinus. Thus, evidence from multiple saurischian clades indicates that the antorbital sinus was well vascularized, and may have been critical to the thermoregulatory strategy of theropods, if not even a much broader group of archosaurs. The allocation of often nearly half of the skull length to a well-vascularized region of the head other than the oral, nasal, or orbital regions, indicates that theropods likely deployed a novel thermoregulatory strategy utilizing the antorbital air sinuses.

Canal for premaxillary vessels. In all of the diapsids sampled, the blood vessels contained within the premaxilla demonstrated consistent patterns. At the caudal aspect of the base of the nasal process of the premaxilla, near the interpremaxillary suture, foramina lead to rostrally directed canals that transmit neurovascular bundles through the premaxilla (Fig. 7) to supply the skin (Oelrich, 1956; Bubień-Waluszewska, 1979; Midtgård, 1984b; Witmer, 1995; Sedlmayr, 2002). This foramen has been described in dinosaur taxa including *Plateosaurus* (Leal, 2004), *Majungasaurus* (Sampson et al., 1996; Sampson and Witmer, 2007), *Sinraptor* (Currie and Zhao, 1993), and *Maiasaura* (Horner, 1983). The medial nasal nerve, a branch of the ophthalmic division of the trigeminal nerve that travels with the medial nasal vessels, is known to pass through this canal in extant diapsids (Oelrich, 1956; Witmer 1995; Sedlmayr, 2002) and based on homology, is likely to do the same in dinosaurs (Sampson and Witmer, 2007; Currie and Zhao, 1993). Several blood vessels are known to anastomose with the premaxillary vessels in extant diapsids. Branches from the lateral nasal vessels (birds, crocodilians, and iguanas), maxillary vessels (crocodilians and iguanas), and palatine vessels (birds, crocodilians, and iguanas) can participate in the formation of the premaxillary vessels (Fig. 7). Therefore, this osteological correlate is not solely for the medial nasal vessels.

Depending on the size of the other participating blood vessels, this canal can, on a weak basis, be interpreted as an osteological correlate for the medial nasal vessels. Because the medial nasal vessels are the primary supply and drainage for internal nasal structures, like respiratory concha (Witmer, 1995; Sedlmayr, 2002; Bourke et al., 2014; Porter and Witmer, 2015, 2016; Porter et al., 2016), an osteological correlate is important to help shed light on the amount of vascularization to the internal nasal region.

Ankylosauria. The two sampled *Euoplocephalus* specimens (AMNH 5403, 5405) have the largest premaxillary canals sampled, 0.54 cm^2 and 1.05 cm^2, respectively (Table 1). These two specimens also demonstrate large canals for the medial and lateral nasal vessels (Witmer and Ridgely, 2008), indicating that the vascularization of the intracapsular nasal region was high, yet the size of the premaxillary canal was much smaller than the medial nasal canal. *Edmontonia* (AMNH 5381) and *Panoplosaurus* (ROM 1215) had the next two largest cross-sectional areas for this canal (Table 1). The smallest ankylosaurid in the sample, the juvenile *Pinacosaurus* (ZPAL MgD-II/1), did not demonstrate clear osteological correlates for the premaxillary vessels. The nodosaurids in the sample demonstrated premaxillary canals that were roughly similar in size to the other measured canals, yet were always smaller than the cerebral carotid canal.

Theropoda. In the largest-headed dinosaur in the sample, *Tyrannosaurus* (FMNH PR 2081), the premaxillary canals were the second smallest canal measured (larger than the cerebral carotid canal), and were much smaller than the palatal or lateral nasal sides of the subnarial foramen (Table 1). This finding indicates that in *Tyrannosaurus*, the vascularization of the narial region was not as high as other dinosaur specimens and may be a product of its plesiomorphically small narial region. In *Majungasaurus* (FMNH PR 2100), the premaxillary canal was the largest canal measured, even larger than the dorsal alveolar canal. *Majungasaurus* is known to lack a subnarial foramen (Sampson et al., 1996; Sampson and Witmer, 2007), and subsequently lost a collateral pathway from the palatine vessels. *Majungasaurus* had premaxillary canals that are about the same size as the juvenile *Tyrannosaurus* (BMR P2002.4.1) (0.24cm^2 and 0.43 cm^2, respectively), which had a similar head volume (Table 1), which may indicate that more blood was flowing through the premaxilla, possibly as a response to the lost connection to the palatine vessels. These findings strongly suggest that the internal structure of the nasal region was not vascularized beyond the necessity of nutrition, and the theropod narial region was probably not an emphasized site of thermal exchange.

Sauropodomorpha. The premaxillary canals of *Plateosaurus* (MB.R.1937) were much smaller than the other canals measured (Table 1) and showed paired dorsal and ventral canals (Fig. 3). Their small size may indicate that the medial nasal vessels likewise were small or that they had supplied all of the blood to the nasal region once they reached the premaxilla and were reduced in size, similar to *Euoplocephalus*. The premaxillary canals were much smaller than the cerebral carotid canal (0.03 cm^2 vs. 0.26 cm^2, respectively; Table 1). The same trend was found in the larger sauropods, with the premaxillary canals being either slightly smaller or the same size as the cerebral carotid canal. The large size of the anastomosis between the nasal and palatine vessels likely overshadowed the premaxillary vessels in these dinosaurs.

Statistical Analysis

Tests for phylogenetic signal using Pagel's λ and Blomberg's K returned values (Table 4) that indicate phylogenetically informed tests were appropriate (Felsenstein, 1985), with some values of λ being between 0.69 and 0.96. The multivariate and pairwise general linear models indicated significant correlation (Table 3) between size parameters (head volume and body mass) and canal cross-sectional areas, indicating that tests robust to multicollinearity must be used. A second correlation test designed to highlight the degree of correlation between each variable (Table 5) also indicated that all of the variables were correlated, especially canals that lead to the anastomosis of the palatine, nasal, maxillary vessels, with the least amount of correlation being found between head volume and cerebral carotid canal cross-sectional area and between the cerebral carotid and dorsal alveolar canal cross-sectional areas. These results indicate that cerebral carotid canal size is less influenced by head volume and that collateral pathways to the nasal and oral regions are less influenced by cerebral carotid canal size.

A multivariate PLS was conducted on the log-transformed data to probe the dataset for correlations between canal size and other size parameters (head volume and body mass; Table 6, Fig. 12A). The first two components explained 100% of the variance in the dataset. The first component explained 90% of the variance and loaded heavily with body mass. The second component explained 10% of the variance and was loaded with head volume. For each canal investigated, the first component explained 75% of the variance in dorsal alveolar canal size, 88% of the variance in palatine canal size, 83% of the variance in premaxillary canal size, 71% of the variance in cerebral carotid canal size, and 85% of the variance in dorsal alveolar canal size. A second PLS regression was conducted (Table 6) and included an investigation of the interaction between head volume and body mass. The first component of this regression loaded heavily with this interaction and explained 99% of the variance in the dataset. These results highlight the dataset's complexity, in that it includes specimens with different combinations of large or small body masses and large or small heads. It also highlights that blood vessels in sites of thermal exchange are responding to multiple pressures. These results are consistent with other known instances of complex interactions between head and body size. For example, in lizards there are cases of positive allometry between body mass and head size in males and negative allometry in females of the same or closely related species (Verwaijen et al., 2002; Kaliontzopoulou et al., 2008), which may explain differences in functional parameters like bite force (Verwaijen et al., 2002). There are similar cases known in dinosaurs, where evidence from *Plateosaurus* indicated negative allometry between head size and body mass (Gunga et al., 2007), whereas Therrien and Henderson (2007) detected a negative allometric relationship between skull length and body length and a positive allometric relationship between skull length and body mass in theropods. Hone et al. (2016) also provided evidence for differing allometric relationships between skull bones in *Prototceratops*. These cases indicate the presence

TABLE 7. Summary of the principal component analyses using the residuals from the pGLS regressing canal size against head volume

	PCA loadings					PVA Eigen vectors				
Canal	PC1	PC2	PC3	PC4	PC5	PC1	PC2	PC3	PC4	PC5
Cerebral carotid	−0.81	−0.50	0.24	−0.17	0.09	**−0.57**	**−0.41**	0.50	−0.39	0.33
Palatal	−0.88	0.09	−0.44	−0.11	0.03	**−0.54**	0.07	−0.80	−0.21	0.11
Lateral nasal	−0.82	0.47	0.11	0.31	−0.01	**−0.56**	0.37	0.23	0.70	−0.03
Premaxillary	−0.56	0.64	0.15	−0.33	−0.39	−0.22	0.29	0.18	−0.43	−0.81
Dorsal alveolar	0.14	0.96	0.07	−0.16	0.13	0.10	**0.78**	0.15	−0.36	0.48
% Variance explained:										
Proportion	0.50	0.37	0.05	0.04	0.02					
Total	0.50	0.88	0.94	0.98	1					
Broken-stick method:										
Proportion	0.48	0.26	0.16	0.09	0.01					
Total	0.48	0.71	0.87	96.0	1					
Guttman-Kaiser Criterion						0.40	0.38	0.37	0.42	0.35

The axis loadings and eigenvectors determine which values load significantly onto each axis. The first two axes (marked in bold under PCA Loadings) are considered significant as they explain 88% of the total variance and are supported by the broken-stick method (Jackson, 1993). Eigenvector values greater than the average of the absolute values of the eigenvectors for each axis indicate significant loadings (Guttman-Kaiser Criterion from Yeomans, 1982) and marked in bold (under Eigenvectors).

of complex influences on skull and body size growth and evolution in each species.

Residuals from the pGLS, which control for the influence of head volume on canal size data, were retested for assumption violations and were found to have variance inflation factors that indicate reduced multicollinearity (Table 5). The first two axes of the pPCA (Table 7) were significant based on the broken-stick method and explained 88% of the variance. PC1 explained 50% of the total variance and loaded heavily with the cerebral carotid, lateral nasal, and palatine canals. PC2 explained 37% of the total variance and was loaded heavily with the dorsal alveolar and cerebral carotid canals. The results of the pPCA largely agree with the anatomical analysis and resolved taxa that had large differences between cross-sectional areas (Fig. 12B). The grouping of species in the right half of the plot in Figure 12B (i.e., all crocodilians, lizards, and *Tyrannosaurus*) indicates species with equivalent canal cross-sectional areas, suggesting that, in particular, the cerebral carotid canal is not larger than necessary to supply the basic nutritional and metabolic needs of the brain and nasal cavity. Of course, these results do include some base thermoregulatory signal, as all of the extant species are known to use cephalic sites of thermal exchange as part of their thermoregulatory strategy. This similarity of canal caliber indicates that these taxa demonstrate a balanced vascular pattern, meaning that none of the canals to sites of thermal exchange were emphasized over the others. In other words, these species were able to supply sites of thermal exchange with a balanced vascular pattern that was part of a distributed rather than a focused thermoregulatory strategy. The taxa found in the center of the plot (Fig. 12B; *Edmontonia* and *Panoplosaurus*) are taxa with large cerebral carotid and palatine canals, yet show smaller dorsal alveolar and lateral nasal canals, respectively. This statistical finding indicates that there is still a balance between supply pathways to sites of thermal exchange, yet canal size is indicating a response to blood flow to sites of thermal exchange. That is, the canals leading to sites of thermal exchange were balanced and of similar value, but the cerebral carotid canal size was large enough to supply these moderately emphasized sites of thermal exchange. Because of the canal size in sites of thermal exchange, these taxa are also considered balanced and still relied on the cerebral carotid vessels to supply a moderately emphasized nasal region. On the other hand, taxa in the upper left region of the plot (*Diplodocus*, *Camarasaurus*, and *Euoplocephalus*) have large nasal, palatal, or dorsal alveolar canals and are regarded as having an unbalanced blood supply and demonstrate emphasized sites of thermal exchange as part of a focused thermoregulatory strategy. The size of the cerebral carotid canal is small, and canals housing collateral blood flow pathways were large, which indicates that the internal carotid system could not supply the emphasized sites of thermal exchange sufficiently and pathways from the external carotid were emphasized to compensate. Anatomically, the taxa in the upper left quadrant have a different combination of large canals. The sauropods have large palatine and nasal canals but small dorsal alveolar canals, and *Euoplocephalus* has large dorsal alveolar and nasal canals but small palatine canals. The way these variables load on each axis is obscuring the anatomical differences between each taxon, which can be detected because the eigenvectors for each significantly loading variable are nearly 90 degrees to one other. The resultant vector points parallel to the *Y*-axis, clumping taxa with vastly different anatomical differences. Yet, anatomically, these large taxa have canals that are very different from each other and the smaller taxa, highlighting the emphasis on each participating blood vessel. These results indicate that the pattern of blood vessels within these canals was unbalanced, meaning that a subset of blood vessels were enlarged and supplied specific sites of thermal exchange. These unbalanced blood vessels were enlarged beyond the basic metabolic needs of the tissues and were responding to thermoregulatory pressures as part of a focused thermoregulatory strategy.

The statistics used were designed to detect the influence of head volume and body mass on canal cross-sectional area and largely support the qualitative anatomical analysis of canal cross-sectional area. Large dinosaur taxa, such

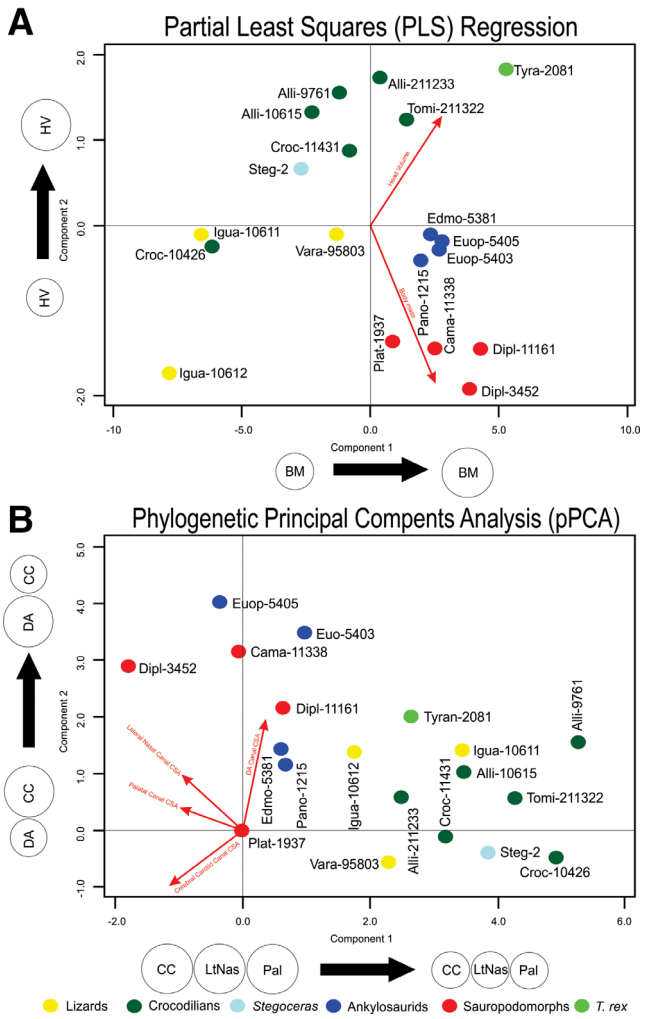

Fig. 12. Biplot of the PLS (**A**) and the pPCA (**B**) analyses. Each axis is labeled with canals that had the highest loading on each axis and circles representing the direction of canal cross-sectional area increase. Red arrows indicate loading vectors representing the direction and magnitude of canals with the highest loadings. Each specimen is labeled with the first four letters of the genus name and specimen number. Abbreviations are found in Table 2. The PLS regression indicated that body mass and head volume have a complex relationship, with the extant sample and *Tyrannosaurus rex* sharing a similar body-mass-to-head-volume ratio, ankylosaurs having a larger body mass than head volume, and sauropods having the largest body-mass-to-head-volume ratio. The relationship between body mass and head volume was found to explain 99% of the variance (Table 6). The pPCA results separated species with balanced (right half of plot) and unbalanced (left half of plot) vascular patterns. *T. rex* was found to reflect similar canal size ratios as found in extant diapsids, indicating a balanced vascular supply and distributed thermoregulatory strategy. Larger-bodied specimens with unbalanced canal sizes were found in the same region of the plot, but anatomically showed different combinations of unbalanced canal sizes that supported focused thermoregulatory strategies. These two analyses indicate that dinosaur blood vessels were responding to complex pressures imposed by large size and that different species often responded by deploying the same blood vessels in different combinations. Abbreviations: CC, cerebral carotid canal; BM, body mass; DA, dorsal alveolar; HV, head volume; LtNas, lateral nasal; Pal, palatine. The size of the circle indicates canal size.

as *Euoplocephalus*, *Diplodocus*, and *Camarasaurus*, all show anatomically emphasized narial regions that had statistically greater blood supply than other taxa in the sample. In these three taxa, the blood supply to the narial region is derived from slightly different sources, indicating a convergence on a similar solution to the common problem of high heat loads. *Tyrannosaurus*, also a large-bodied taxon, had an anatomically plesiomorphic narial region and also was found to have had a statistically similar amount of blood flow to the nasal region relative to head volume as do extant taxa. Thus, *Tyrannosaurus*, despite its large body mass, did not seem to emphasize sites of thermal exchange more than extant taxa.

DISCUSSION

Our anatomical analysis revealed insights into dinosaur thermoregulatory strategies and is a significant step forward in the understanding of dinosaur physiology. Large-bodied dinosaurs (e.g., *Camarasaurus*, *Euoplocephalus*, and *Tyrannosaurus*) had surface-to-volume ratios that would have slowed the shedding of heat and required physiological mechanisms to deal with potentially dangerously high heat loads. Vascular evidence gathered from extant and extinct diapsids supports the hypothesis that dinosaurs emphasized certain sites of thermal exchange to play a thermoregulatory role in buffering neurosensory tissues from thermal extremes. Vascular evidence in fossils reveals that both large-headed and small-headed dinosaurs shared branching patterns similar to extant diapsids (Porter, 2015; Porter and Witmer, 2015, 2016; Porter et al., 2016). Modifications to this plesiomorphic vascular pattern become clear when the cross-sectional areas of canals housing blood vessels are compared statistically. Evidence from multiple dinosaur clades indicates shifts in vascular patterns from small to large body sizes (and hence head sizes). Small-headed dinosaurs show a modest dorsal alveolar canal that usually exits the maxilla before the anastomosis with the nasal and palatine vessels. Evidence for the anastomosis between the nasal, palatine, and maxillary vessels indicates that all three of these blood vessels are of relatively equal size, and suggests balanced blood flow between them. The cerebral carotid canal was about the same size or slightly larger than the other measured canals and was likely able to supply the nasal region, which is the primitive diapsid condition. The dorsal alveolar canal in large-headed dinosaurs usually coursed through the maxilla to the premaxilla and into canals that housed the nasal, palatine, maxillary vessel anastomosis. This shift from an external anastomosis (i.e., closer to the surface of the skull) to a more internal anastomosis (i.e., recessed within the narial fossa) may reflect a shift in vascular anatomy as dinosaurs achieved greater sizes. Many large-bodied dinosaurs demonstrate expanded narial regions that were around half the length of the skull (Witmer, 2001). These emphasized regions contain enlarged canals, such as the dorsal alveolar canal in *Euoplocephalus* and the subnarial foramen in *Camarasaurus*. This evidence for the nasal, palatine, and maxillary vessel anastomosis in large dinosaurs suggests that as dinosaur size and need for thermoregulatory ability increased, collateral blood flow also increased, which resulted in the emphasis of one or two, but not all three blood vessels forming the anastomosis.

Large-headed dinosaurs had a cerebral carotid canal that was nearly the same size as that in small-headed dinosaurs, which indicates that in large dinosaurs, the cerebral carotid supplied just the brain and was not of a large-enough caliber to also supply an emphasized nasal region. In these species, the branches of the external carotid artery then served as an important collateral blood supply to expanded narial regions. An exception to this pattern was found in nodosaurids. *Edmontonia*, a dinosaur that had a slightly smaller head volume than *Euoplocephalus*, had a cerebral carotid canal that not only was the second largest in the sample (at 0.48 cm^2) but also was larger than all its other measured canals and appeared to be very balanced. Instead of increasing collateral blood flow, *Edmontonia* increased the cerebral carotid canal to supply the narial region as extant diapsids do. It is not clear how *Edmontonia* was able to escape the constraint seemingly imposed on the other dinosaurs in the sample.

Ankylosaurs such as *Panoplosaurus* and *Euoplocephalus* had long and convoluted airways with large dorsal alveolar and nasal canals (Witmer and Ridgely, 2008; Bourke et al., 2018), yet showed reduced vasculature to the palatal region. This finding suggests that the narial region, but not the oral region, likely held a central role in modulating head temperatures. The size of the maxillary vessels indicates that they are a main collateral route of blood supply to the narial region, but the palatine vessels are not. The dorsal alveolar canal is large, yet there is little evidence on the lateral aspect of the maxilla to indicate enhanced sensation or trigeminal nerve enlargement. Therefore, the maxillary nerve is likely not the driving force behind the expanded canals and indicates that most of the canal is reserved for blood vessels. The large osteological correlates for the nasal vessels may also indicate that a large amount of cooled venous blood passed through the nasal region. Thus, blood from the maxillary vessels flowed into the nasal region where it was cooled by evaporative cooling, and then large nasal veins carried cooled blood caudally toward neurosensory tissues. Recent computational fluid dynamic research into the airflow and heat exchange abilities of *Euoplocephalus* and *Panoplosaurus* (Bourke et al., 2018) has indicated that the convoluted nasal passages had the ability to exchange heat. This finding, in conjunction with the vascular data presented here, strongly suggests that *Euoplocephalus* and *Panoplosaurus* are using the nasal cavity for thermoregulation of cephalic neurosensory tissues like the brain, and that these canals were enlarged to accommodate increased blood flow, which is consistent with the lack of any evidence for significant trigeminal nerve expansion. These two dinosaurs, to date, offer the strongest data that support the hypothesis for a focused thermoregulatory strategy sustained by an unbalanced pattern of blood vessels.

Evidence in sauropods indicates that large blood vessels passed through the large subnarial foramen between the expanded narial region and the oral region, which implies that both regions were well vascularized, yet the maxillary vessels were much smaller and likely provided a minor amount of blood to the nasal region. It should again be noted that the subnarial foramen does not transmit any nerves along with the palatonasal vascular anastomosis in extant diapsids and thus can be safely interpreted as being essentially exclusively vascular in extinct dinosaurs, as well. The available vascular evidence suggests that sauropods likely had a vast palatal vascular plexus in the oral region that would have shed heat and added another site of thermal exchange, along with the nasal region, to their focused thermoregulatory strategy. Sauropods differed from ankylosaurs by including the oral region as a site of thermal exchange and by supplying the nasal region via the palatine vessels instead of the maxillary vessels (Fig. 13).

Theropods demonstrated a balanced pattern of blood supply and typically retained a plesiomorphically small narial region. Theropods with large body masses were under the same thermal constraints as other large dinosaurs and likely needed to shed heat to buffer neurosensory tissues. Evidence shown here, however, indicates that theropods may not have had a "typical" thermoregulatory strategy with enhanced blood supply to one or more of the three main sites of thermal exchange. The emphasized narial region of *Euoplocephalus*, about 850 cm^3 in volume (Witmer and Ridgely, 2008), had approximately the same blood flow based on canal cross-sectional area as does *Tyrannosaurus*, with a nasal region volume of 10,750 cm^3 (Witmer and Ridgely, 2008). This comparison shows the difference between a plesiomorphic balanced vascular pattern in theropods and an unbalanced vascular pattern in a dinosaur species with a focused thermoregulatory strategy (*Euoplocephalus*) that emphasized the narial region. Theropods do, however, have an alternative and novel thermoregulatory candidate, which is the paranasal sinus system that shows evidence for vascularization of the antorbital air sinus. Large theropods like *Carcharodontosaurus* and *Tyrannosaurus* show ample evidence for blood vessels entering and leaving the antorbital sinus in part simply because larger animals in general tend to show osteological correlates of all soft tissues more prominently. *Rugops* and *Majungasaurus*, which are smaller dinosaurs, however, show even more evidence for vascularization of the air sinus, but in this case due to their apomorphic hypermineralization of the dermis that produces the remarkable surface rugosity that records the presence of vessels that likely were widely present in theropods (Sereno et al., 2004; Sampson and Witmer, 2007). Smaller theropods show more subtle evidence for the vessels supplying the antorbital sinus in part simply because of their small size and the scaling of the intensity of osteological correlates, but also perhaps because their higher surface-to-volume ratios resulted in lower likelihood of overheating. In general, all of the bones surrounding the antorbital sinus in species from diverse theropod clades show evidence for the extensive vascularization of the antorbital sinus. Therefore, theropods could have deployed a large amount of blood over the exposed lateral surface of the antorbital sinus. Using the air sinus as a well vascularized and actively ventilated surface to facilitate evaporative or radiative cooling would have had a similar effect as deploying the oral or nasal region as a site of thermal exchange. Modern archosaurs, like birds, are known to deploy the oral, nasal, and orbital regions in their thermoregulatory strategies, but the thermoregulatory status of avian paranasal sinus systems has not received a comparable level of scrutiny from physiologists. The plesiomorphic morphology of the oral and narial regions and expanded paranasal sinus system in large-headed extinct theropods supports the hypothesis that theropods used the antorbital air sinus as part of a focused thermoregulatory strategy not previously recognized in any other vertebrate clade but worthy of consideration for other groups of archosaurs.

The results of the statistical analysis, using both pPCA and PLS, clearly showed that canals conveying blood to sites

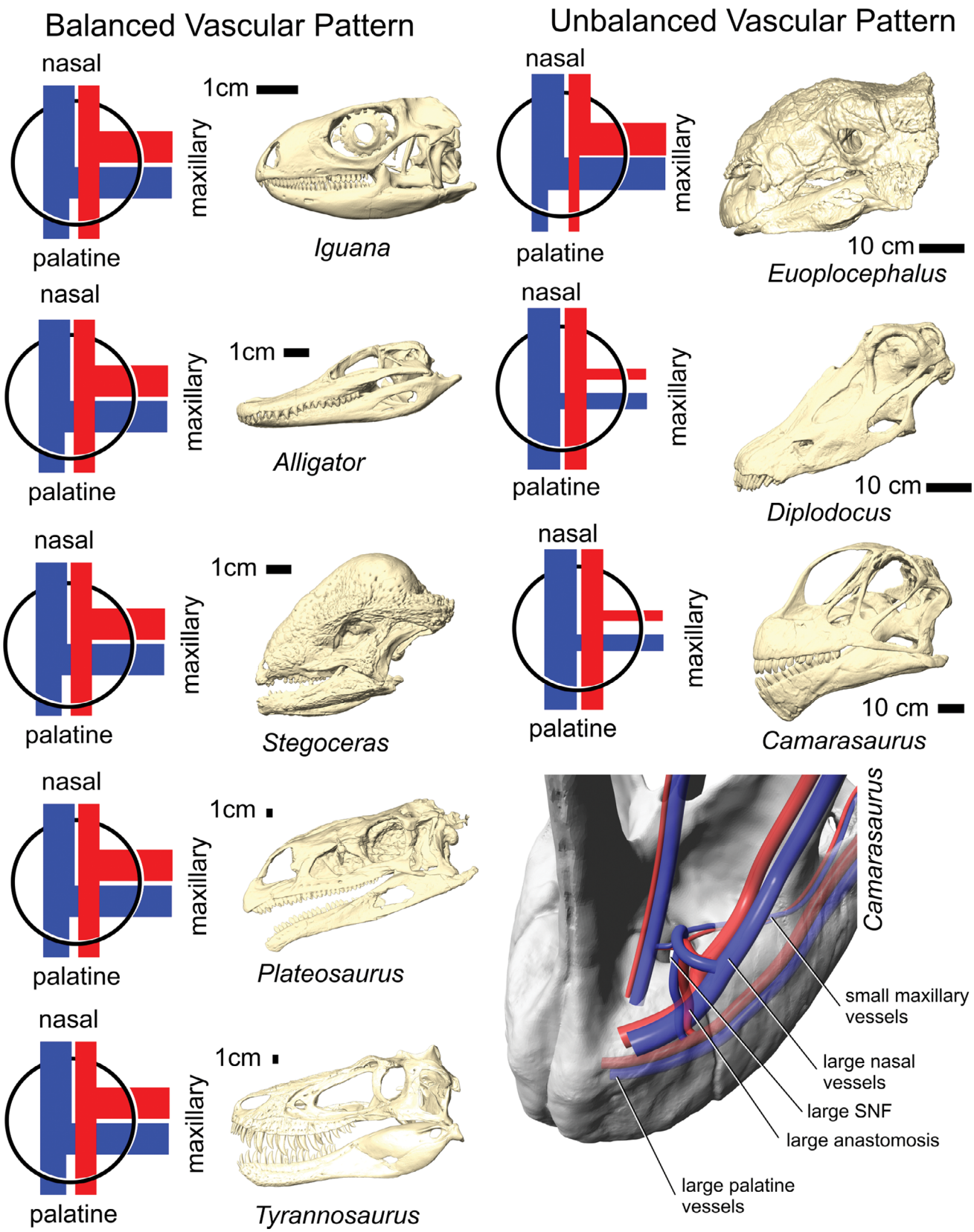

Fig. 13. Smaller-headed species and theropods were found to have a balanced pattern of canal sizes indicating roughly comparable levels of vascular supply to the three main sites of thermal exchange (nasal, oral, and orbital regions), that is, a distributed thermal strategy. The species with unbalanced patterns of vascular supply had sets of canals that would have contributed a larger proportion of blood flow to the oral or nasal region, which is indicative of emphasized sites of thermal exchange and a focused thermal strategy.

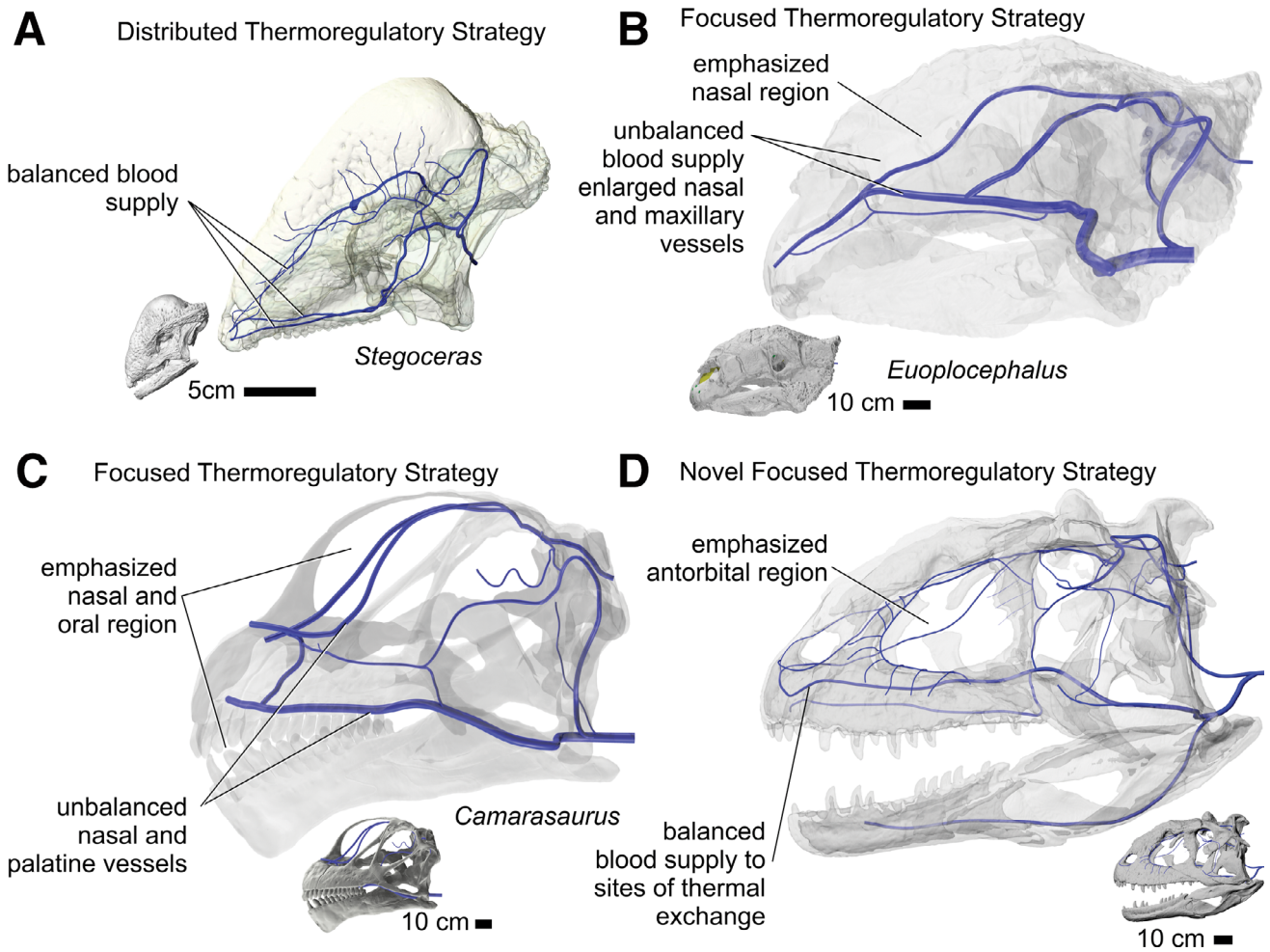

Fig. 14. Different dinosaur clades varied with regard to whether the vascular supply to the three main sites of thermal exchange observed in extant diapsids (nasal, oral, and orbital regions) displayed a balanced or unbalanced pattern of vascular supply, with the former reflecting a distributed thermoregulatory strategy (roughly equivalent roles for each site of thermal exchange) and the latter reflecting a focused strategy (wherein one or two sites were emphasized over the others). Dinosaurs with large body masses tended to evolve focused thermoregulatory strategies to enhance venous cooling of blood destined for structures associated with the neurosensory tissues of the brain and eyes. (**A**) *Stegoceras* (UALVP 2), a small-bodied pachycephalosaurian dinosaur, had plesiomorphically moderate sites of thermal exchange with evidence for a balanced pattern of blood flow, no emphasis of any particular sites of thermal exchange, and thus a distributed thermoregulatory strategy. (**B**) *Euoplocephalus* (AMNH 5405) had a highly expanded narial airway with evidence for increased blood flow and an unbalanced vascular pattern emphasizing the nasal region over other sites, resulting in a focused thermoregulatory strategy. (**C**) *Camarasaurus* (GMNH PV 101) shows evidence for an unbalanced vascular pattern with increased blood flow to the oral and especially the nasal regions, again resulting in a focused thermoregulatory strategy. (**D**) *Majungasaurus* (FMNH PR 2100) plesiomorphically retained a balanced pattern of blood supply to the three main sites of thermal exchange, but the antorbital cavity was expanded with evidence of a rich blood supply to the antorbital paranasal air sinus, suggesting a novel form of a focused thermoregulatory strategy not observed in extant diapsids. Different dinosaur clades exhibit different thermoregulatory strategies while utilizing homologous blood vessels. These examples highlight the differing thermoregulatory strategies in dinosaurs, with (B) and (C) converging on the nasal region and (D) apomorphically emphasizing the paranasal sinuses.

of thermal exchange were emphasized in clades with large head volumes and body masses. The PLS and pPCA were deployed to detect and correct, respectively, for the influence of head volume and body mass on canal cross-sectional area, resulting in an equivalent comparison between dinosaurs with large and small head volumes. The PLS detected the influence of body size on canal size and indicated that the interaction between head volume and body size is complex. The anatomical analysis confirmed this finding in species with different head-volume-to-body-mass ratios. In the pPCA, the dinosaurs with unbalanced vascular patterns were clearly separated from those with balanced patterns (Fig. 12), indicating that there is a clear difference in thermoregulatory strategies between dinosaurs with large head volumes and body sizes. By controlling the effects of head volume on canal size, the blood flow associated with basic nutritional demands was isolated, and the effects of body mass on sites of thermal exchange became clear. The blood vessels sized beyond the requirements of tissue nutritional demands were responding to some kind of physiological pressure, which we hypothesize relate to high heat loads. Both statistical tests, one with phylogenetic correction and one without, show similar results indicating that the convergent evolution of an emphasized narial region resulted from

the biophysical demands that large size places on physiological thermoregulatory systems.

The convergent evolution of expanded narial, oral, and antorbital regions with evidence for enhanced blood flow highlights the importance of physiological thermoregulation in large dinosaurs (Fig. 14). The large body sizes would have caused neurosensory tissues like the brain and eyes to experience increased temperatures, which would have had not only a performance cost but also would have led to operating close to lethal temperatures. Many ecological and biophysical models (Seebacher, 2003; Gillooly et al., 2006) indicate that large dinosaurs could have had body temperatures close to and above lethal levels for extant taxa. Isotopic analyses (Eagle et al., 2011) show that dinosaurs had head temperatures a few degrees cooler than expected for their core body temperature. This evidence shows that at least some (but perhaps all) dinosaurs could have established and maintained a head-to-body temperature differential, just as extant taxa do, by utilizing blood vessels within sites of thermal exchange (Crawford, 1977; Midtgård, 1984a; Spray and Belkin, 1973; Spotila et al., 1977; Borrell et al., 2005). This pattern, shown in so many extant diapsids, was likely an important ability in large dinosaurs.

Archosaurs are one of the most diverse and morphologically disparate terrestrial vertebrate clades in all of Earth's history. By examining the physiological processes of extant archosaurs and finding osteological correlates, we can shed light on physiological processes and thermoregulatory strategies in dinosaurs. The evidence presented here shows that as large body size evolved, the cephalic vasculature also evolved to support a physiological thermoregulatory role within emphasized sites of thermal exchange. Small-bodied dinosaurs in the same clade as large-bodied dinosaurs showed no evidence for emphasized vascular sites, whereas intermediate-sized dinosaurs showed the beginnings of vascular enhancement, and the larger dinosaurs showed clear evidence for enhanced blood flow to sites of thermal exchange. The evidence indicates a convergent response to large size and thermal issues, with dinosaurs often emphasizing different regions of the head—as well as the blood vessels within—to solve the biophysical limitations that great size imposes.

Given the labor-intensive nature of the data collection for this project, coupled with the requirement of CT-scan datasets of often-large fossil specimens, the study presented here was of necessity limited in scope, both intraspecifically and across clades of dinosaurs. Future directions include sampling other clades, with Ornithopoda and Ceratopsia both presenting interesting examples of independent evolution of large body sizes as well as large (often enormous) head sizes within each clade. Likewise, the recruitment of the antorbital cavity by theropods as a novel site of heat exchange requires more attention, including extending the analysis outside Dinosauria to other archosaur groups with large antorbital cavities.

AUTHOR CONTRIBUTIONS

W.R.P. and L.M.W. conceived and designed the experiments. W.R.P. performed the experiments. W.R.P. and L.M.W. analyzed the data. W.R.P. and L.M.W. contributed reagents/materials/analysis tools. W.R.P. and L.M.W. wrote the paper.

ACKNOWLEDGEMENTS

Thanks to J. Bourke, E. Caggiano, D. Cerio, D. Dufeau, C. Early, T. Hieronymus, C. Holliday, D. Kincaid, A. Morhardt, P. O'Connor, R. Ridgely, K. Slepchenko, E. Snively, and T. Wilson for assistance, insightful comments, and discussions. Thanks to museums, curators, and collections managers that allowed access to dinosaur fossils and CT scanning, including Paul Sereno and Bob Masek (University of Chicago); Mark Norell and Carl Mehling (AMNH); Matthew Lamanna, David Berman, and Amy Henrici (CM); Peter Makovicky and William Simpson (FMNH); Matthew Carrano and Michael Brett-Surman (USNM); Jacques Gauthier and Daniel Brinkman (YPM); Kevin Padian and Patricia Holroyd (UCMP); and Randall Irmis (NHMU). We thank Jessica Maisano (University of Texas, Austin) for providing access to unpublished CT-scan data of *Varanus komodoensis*. Many thanks to Donald Miles, Ashley Morhardt, Ryan Felice, and Eric Gorscak for statistical guidance and discussion. Thanks to Victoria Arbour, Brandon Hedrick, and an anonymous reviewer who provided comments that resulted in a much-improved manuscript. W.R.P. acknowledges support from Ohio University (OU) Student Enhancement Award, Jurassic Foundation Grant-in-aid of Research, Ohio Center for Ecology and Evolutionary Studies Research Fellowship, OU Heritage College of Osteopathic Medicine, OU Graduate Student Senate Grant-in-aid of Research, Sigma Xi Grant-in-aid of Research, and the University of California Welles Fund. L.M.W. additionally acknowledges support from the United States National Science Foundation (NSF IOB-0517257, IOS-1050154, and IOS-1456503). The funders had no role in study design, data collection and analysis, decision to publish, or preparation of the manuscript.

LITERATURE CITED

Arad Z, Marder J. 1982. Comparative thermoregulation of four breeds of fowls (*Gallus domesticus*), exposed to a gradual increase of ambient temperatures. Comp Biochem Physiol A72A: 179–184.

Arad Z, Midtgård U. 1984. Differences in the structure of the rete ophthalmicum among three breeds of domestic fowls, *Gallus Gallus domesticus* (Aves). Zoomorphology 104:184–187.

Arbour VM, Burns ME, Sissons RL. 2009. A redescription of the ankylosaurid dinosaur *Dyoplosaurus acutosquameus* Parks, 1924 (Ornithischia: Ankylosauria) and a revision of the genus. J Vertr Paleontol 29:1117–1135.

Arbour VM, Currie PJ. 2013. *Euoplocephalus tutus* and the diversity of Ankylosaurid dinosaurs in the Late Cretaceous of Alberta, Canada, and Montana, USA. PLoS ONE 8:e62421.

Barker CT, Naish D, Newham E, Katsamenis OL, Dyke G. 2017. Complex neuroanatomy in the rostrum of the Isle of Wright theropod *Neovenator salerii*. Sci Rep UK 7:3749. https://doi.org/10.1038/s41598-017-03671-3.

Baumel JJ. 1975. Aves: heart and blood vessels. In: Getty R, editor. *Sisson and Grossman's the anatomy of the domestic animals*. Philadelphia: W.B. Saunders. p 1968–2003.

Baumel JJ. 1993. Systema cardiovasculare. In: Baumel JJ, editor. *Handbook of avian anatomy: nomina anatomica avium*. Cambridge: Nuttall Ornithological Club. p 407–476.

Bell MA, Braddy SJ. 2012. Cope's rule in the Ordovician trilobite Family Asaphidae (Order Asaphida): patterns across multiple most parsimonious trees. Hist Biol 24:223–230.

Benson RBJ, Hunt G, Carrano MT, Campion N. 2018. Cope's Rule and the adaptive landscape of dinosaur body size evolution. Palaeontology 61:13–48.

Berman DS, McIntosh JS. 1978. Skull and relationships of the Upper Jurassic sauropod *Apatosaurus* (Reptilia, Saurischia). Bull Carnegie Mus Nat Hist 8:1–35.
Berner D. 2011. Size correction in biology: how reliable are approaches based on (common) principal component analysis? Oecologia 166:961–971.
Blomberg SP, Garland T, Ives AR. 2003. Testing for phylogenetic signal in comparative data: behavioral traits are more labile. Evolution 57:717–745.
Borrell BJ, LaDue TJ, Dudley R. 2005. Respiratory cooling in rattlesnakes. Comp Biochem Physiol A 140:471–476.
Bourke JB, Porter WR, Ridgely RM, Lyson TL, Schachner ER, Bell PR, Witmer LM. 2014. Breathing life into dinosaurs: tackling challenges of soft-tissue restoration and nasal airflow in extinct species. Anat Rec 297:2148–2186.
Bourke JM, Porter WR, Witmer LM. 2018. Convoluted nasal passages function as efficient heat exchangers in ankylosaurs (Dinosauria: Ornithischia: Thyreophora). PLoS ONE 13:e0207381.
Brochu CA. 2003. Osteology of *Tyrannosaurus rex*: insights from a nearly complete skeleton and high-resolution computed tomographic analysis of the skull. J Vertebr Paleontol 22:1–138.
Brooke MDL, Hanley S, Laughlin SB. 1999. The scaling of eye size with body mass in birds. Proc R Soc Lond 266:405–412.
Bubień-Waluszewska A. 1979. The cranial nerves. In: King AS, McClelland J, editors. *Form and function of birds, Volume 11*. New York: Academic Press. p 385–438.
Burda DJ. 1969. Developmental aspects of intracranial arterial supply in the alligator brain. J Comp Neurol 135:369–380.
Butler RJ, Upchurch P, Norman DB. 2008. The phylogeny of the ornithischian dinosaurs. J Syst Paleontol 6:1–40.
Campione NE, Evans DC. 2012. A universal scaling relationship between body mass and proximal limb bone dimensions in quadrupedal terrestrial tetrapods. BMC Biol 10:60.
Colbert EH, Cowles RB, Bogert CM. 1946. Temperature tolerances in the American alligator and their bearing on the habits, evolution, and extinction of the dinosaurs. Bull Am Mus Nat Hist 86:331–373.
Cowles RB, Bogert CM. 1944. A preliminary study of the thermal requirements of desert reptiles. Bull Am Mus Nat Hist 83:261–296.
Crawford EC, Palomeque J, Barber BJ. 1977. A physiological basis for head-body temperature differences in a panting lizard. Comp Biochem Physiol A 56A:161–163.
Currie PJ, Zhao XJ. 1993. A new carnosaur (Dinosauria, Theropoda) from the Jurassic of Xinjiang, People's Republic of China. Can J Earth Sci 30:2037–2081.
Delcourt R. 2018. Ceratosaur palaeobiology: new insights on evolution and ecology of the southern rulers. Sci Rep UK 8:9730. https://doi.org/10.1038/s41598-018-28154-x.
Dzialowski EM, O'Connor MP. 1999. Utility of blood flow to the appendages in physiological control of heat exchange in reptiles. J Therm Biol 24:203–222.
Eagle RA, Tütken T, Martin TS, Tripati AK, Fricke HC, Connely M, Eiler JM. 2011. Dinosaur body temperatures determined from isotopic (13C-18O) ordering in fossil biominerals. Science 333:443–445.
Edwards GP, Webb GJ, Manolis SC, Mazanov A. 2017. Morphometric analysis of the Australian freshwater crocodile (*Crocodylus johnstoni*). Aust J Zool 65:97–111.
Felsenstein J. 1985. Phylogenies and the comparative method. Am Nat 125:1–15.
Fowler DW. 2017. Revised geochronology, correlation, and dinosaur stratigraphic ranges of the Santonian-Maastrichtian (Late Cretaceous) formations of the Western Interior of North America. PLoS ONE 12:e0188426.
Galton PM. 2010. Species of plated dinosaur Stegosaurus (Morrison Formation, Late Jurassic) of western USA: new type species designation needed. Swiss J Geosci 103:187–198.
Gauthier JA. 1986. Saurischian monophyly and the origin of birds. In: Padian K, editor. *The origin of birds and the evolution of flight*. San Francisco: The Academy. p 1–55.
George ID, Holliday CM. 2013. Trigeminal nerve morphology in *Alligator mississippiensis* and its significance for crocodyliform facial sensation and evolution. Anat Rec 296:670–680.
Gillooly JF, Allen AP, Charnov EL. 2006. Dinosaur fossils predict body temperature. PLoS ONE 4:e248. https://doi.org/10.1371/journal.pbio.0040248.
Gillooly JJ. 2013. Hotter is Smarter: The temperature-dependence of brain size in vertebrates (No. e155v1). PeerJ PrePrints.
Gilmore CW. 1914. Osteology of the armored Dinosauria in the United States National Museum: with special reference to the genus *Stegosaurus*. Bull US Mus Nat Hist 89:1–136.
Gradstein F, Ogg J. 2004. Geologic time scale 2004—why, how, and where next! Lethaia 37:175–181.
Graham MH. 2003. Confronting multicollinearity in ecological multiple regression. Ecology 84:2809–2815.
Guderley H, Seebacher F. 2011. Thermal acclimation, mitochondrial capacities and organ metabolic profiles in a reptile (*Alligator mississippiensis*). J Comp Physiol B 181:53–64.
Gunga HC, Suthau T, Bellmann A, Friedrich A, Schwanebeck T, Stoinski S, Trippel T, Kirsch K, Hellwich O. 2007. Body mass estimations for *Plateosaurus engelhardti* using laser scanning and 3D reconstruction methods. Naturwissenschaften 94:623–630.
Gutiérrez-Ibáñez C, Iwaniuk AN, Wylie DR. 2009. The independent evolution of the enlargement of the principal sensory nucleus of the trigeminal nerve in three different groups of birds. Brain Behav Evol 74:280–294.
Haenlein M, Kaplan AM. 2004. A beginner's guide to partial least squares analysis. Understand Stat 3:283–297.
Hedrick BP, Chunling C, Omar GI, Fengjiao X, Caizhi S. 2014. The osteology and taphonomy of a *Psittacosaurus* bonebed assemblage of the Yixian Formation (Lower Cretaceous), Liaoning, China. Cretaceous Res 51:321e340.
Heinicke MP, Greenbaum E, Jackman TR, Bauer AM. 2012. Evolution of gliding in southeast Asian geckos and other vertebrates is temporally congruent with dipterocarp forest development. Biol Lett 8:994–997.
Hill RV, Witmer LM, Norell MA. 2003. A new specimen of *Pinacosaurus grangeri* (Dinosauria: Ornithischia) from the Late Cretaceous of Mongolia: ontogeny and phylogeny of ankylosaurs. Am Mus Novit 3395:1–29.
Hocknull SA, Piper PJ, van den Bergh GD, Due RA, Morwood MJ, Kurniawan I. 2009. Dragon's paradise lost: palaeobiogeography, evolution and extinction of the largest-ever terrestrial lizards (varanidae). PLoS ONE 4:e7241.
Holliday CM, Witmer LM. 2007. Archosaur adductor chamber evolution: integration of musculoskeletal and topological criteria in jaw muscle homology. J Morphol 268:457–484.
Hone SWE, Wood D, Knell EJ. 2016. Positive allometry for exaggerated structures in the ceratopsian dinosaur *Protoceratops andrewsi* supports socio-sexual signaling. Palaeontol Electron 19.1:1–13.
Horner JR. 1983. Cranial osteology and morphology of the type specimen of *Maiasaura peeblesorum* (Ornithischia:Hadrosauridae), with discussion of its phylogenetic position. J Vert Paleontol 3:29–38.
Hurum JH, Sabat K. 2003. Giant theropod dinosaurs from Asia and North America: skulls of *Tarbosaurus bataar* and *Tyrannosaurus rex* compared. Acta Palaeontol Pol 48:161–190. https://doi.org/10.26879/338.
Ibrahim N, Sereno PC, Dal Sasso C, Maganuco S, Fabbri M, Martill DM, Zouhir Z, Myhrvold N, Iurino DA. 2014. Semiaquatic adaptations in a giant predatory dinosaur. Science 345:1613–1616.
Irschick DJ, Austin CC, Petren K, Fisher RN, Losos JB, Ellers O. 1996. A comparative analysis of clinging ability among pad-bearing lizards. Biol J Linn Soc 59:21–95.
Jackson DA. 1993. Stopping rules in principal components analysis: a comparison of heuristical and statistical approaches. Ecology 74: 2204–2214.
Jamnickzy H, Russell AP. 2004. Cranial arterial foramen diameter in turtles: a quantitative assessment of size-dependent phylogenetic signal. Anim Biol 54:417–436.
Jungers WL, Pokempner AA, Kay RF, Cartmill M. 2003. Hypoglossal canal size in living hominoids and the evolution of human speech. Hum Biol 75:473–484.
Kaliontzopoulou A, Carretero MA, Llorente GA. 2008. Head shape allometry and proximate causes of head sexual dimorphism in

Podarcis lizards: joining linear and geometric morphometrics. Biol J Linn Soc 93:111–124.
Kendeigh SC. 1969. Energy responses of birds to their thermal environments. Wilson Bull 81:441–449.
Krause DW, Sampson SD, Carrano MT, O'Connor PM. 2007. Overview of the history of the discovery, taxonomy, phylogeny, and biogeography of *Majungasaurus crenatissimus* (Theropoda: Abelisauridae) from the Late Cretaceous of Madagascar. J Vert Paleontol 27:1–20.
Leahey LG, Molnar RE, Carpenter K, Witmer LM, Salisbury SW. 2015. Cranial osteology of the ankylosaurian dinosaur formerly known as *Minmi* sp. (Ornithischia: Thyreophora) from the Lower Cretaceous Allaru Mudstone of Richmond, Queensland, Australia. PeerJ 3:e1475.
Leal LA, Azevedo SAK, Kellner AWA, Da Rosa AAA. 2004. A new early dinosaur (Sauropodomorpha) from the Caturrita Formation (Late Triassic), Paraná Basin, Brazil. Zootaxa 690:1–24.
Malone CL, Reynoso VH, Buckley L. 2017. Never judge an iguana by its spines: Systematics of the Yucatan spiny tailed iguana, *Ctenosaura defensor* (Cope, 1866). Mol Phylogenet Evol 115:27–39.
Maryańska T. 1977. Ankylosauridae (Dinosauria) from Mongolia. Palaeontol Pol 37:85–151.
McIntosh JS, Berman DS. 1975. Description of the palate and lower jaw of the sauropod dinosaur *Diplodocus* (Reptilia: Saurischia) with remarks on the nature of the skull of *Apatosaurus*. J Paleontol 49: 187–199.
Mevik BH, Wehrens R. 2007. The pls package: principal component and partial least squares regression in R. J Stat Softw 18:1–24.
Midtgård U. 1984a. Blood vessels and the occurrence of arteriovenous anastomoses in the cephalic heat loss areas of mallards, *Anas platyrhynchos* (Aves). Zoomorphology 104:323–335.
Midtgård U. 1984b. The blood vascular system in the head of the herring gull (*Larus argentatus*). J Morphol 179:135–152.
Miyashita T, Arbour VM, Witmer LM, Currie PJ. 2011. The internal cranial morphology of an armoured dinosaur *Euoplocephalus* corroborated by X-ray computed tomographic reconstruction. J Anat 219:661–675.
Muchlinski MN. 2008. The relationship between the infraorbital foramen, infraorbital nerve, and maxillary mechanoreception: implications for interpreting the paleoecology of fossil mammals based on infraorbital foramen size. Anat Rec 291:1221–1226.
Muchlinski MN, Deane AS. 2014. The interpretive power of infraorbital foramen area in making dietary inferences in extant apes. Anat Rec 297:1377–1384.
O'Connor MP, Dodson P. 1999. Biophysical constraints on the thermal ecology of dinosaurs. Paleobiology 25:341–368.
Oaks JR. 2011. A time-calibrated species tree of Crocodylia reveals a recent radiation of the true crocodiles. Evolution 65:3285–3297.
Oelrich TM. 1956. The anatomy of the head of *Ctenosaura pectinata* (Iguanidae). Misc Publ Mus Zool Univ Mich 94:1–122.
Pagel M. 1999. Inferring the historical patterns of biological evolution. Nature 401:877–884.
Paradis E, Claude J, Strimmer K. 2004. APE: analyses of phylogenetics and evolution in R language. Bioinformatics 20: 289–290.
Penkalski P. 2014. A new Ankylosaurid from the Late Cretaceous Two Medicine Formation of Montana, USA. Acta Palaeontol Pol 59: 617–634.
Peres-Neto PR, Jackson DA, Somers KM. 2003. Giving meaningful interpretation to ordination axes: assessing loading significance in principal component analysis. Ecology 84:2347–2363.
Pinheiro J, Bates D, DebRoy S, Sarker D, the R Development Core Team. 2013. nlme: linear and nonlinear mixed effects models. R package version 3.1-117. Available at: http://CRAN.R-project.org/package=nlme.
Porter WR. 2015. *Physiological implications of dinosaur cephalic vascular systems*. (PhD Dissertation). Athens, OH: Ohio University.
Porter WR, Sedlmayr JC, Witmer LM. 2016. Vascular patterns in the heads of crocodilians blood vessels and sites of thermal exchange. J Anat 229:800–824.
Porter WR, Witmer LM. 2015. Vascular patterns in iguanas and other squamates: blood vessels and sites of thermal exchange. PLoS One 10:e0139215. https://doi.org/10.1371/journal.pone.0139215.
Porter WR, Witmer LM. 2016. Avian cephalic vascular anatomy, sites of thermal exchange, and the rete ophthalmicum. Anat Rec 299:1461–1486.
Prieto-Márquez A, Norell MA. 2011. Redescription of a nearly complete skull of *Plateosaurus* (Dinosauria: Sauropodomorpha) from the Late Triassic of Trossingen (Germany). Am Mus Novit 3727:1–58.
R Core Team. 2018. *R: A language and environment for statistical computing*. Vienna, Austria: R Foundation for Statistical Computing. https://www.R-project.org/.
Revell LJ. 2012. phytools: an R package for phylogenetic comparative biology (and other things). Methods Ecol Evol 3:217–223.
Rosipal R, Krämer N. 2006. Overview and recent advances in partial least squares. *Subspace, latent structure and feature selection*. New York: Springer Berlin Heidelberg. p 34–51.
Royo-Torres R, Upchurch P, Mannion PD, Mas R, Cobos A, Gascó F, Alcalá L, Sanz JL. 2014. The anatomy, phylogenetic relationships, and stratigraphic position of the Tithonian–Berriasian Spanish sauropod dinosaur *Aragosaurus ischiaticus*. Zool J Linnaean Soc 171:623–655.
RStudio Team. 2015. *RStudio: integrated development for R*. Boston, MA: RStudio, Inc. http://www.rstudio.com/.
Sampson SD, Krause DW, Dodson P, Forster CA. 1996. The premaxilla of *Majungasaurus* (Dinosauria: Theropoda), with implications for Gondwanan paleobiogeography. J Vert Paleontol 16:601–605.
Sampson SD, Witmer LM. 2007. Craniofacial anatomy of *Majungasaurus crenatissimus* (Theropoda: Abelisauridae) from the Late Cretaceous of Madagascar. J Vert Paleontol 27:32–104.
Schulte-Hostedde A, Zinner B, Millar JS, Hickling G. 2005. Restitution of mass size residuals validating body condition indices. Ecology 86:155–163.
Sedlmayr JC. 2002. *Anatomy, evolution, and functional significance of cephalic vasculature in Archosauria*. (PhD Dissertation). Athens, OH: Ohio University.
Seebacher F. 2003. Dinosaur body temperatures: the occurrence of endothermy and ectothermy. Paleobiology 29:105–122.
Seebacher F, Grigg GC, Beard LA. 1999. Crocodiles as dinosaurs: behavioral thermoregulation in very large ectotherms leads to high and stable body temperatures. J Exp Biol 202:77–86.
Senter P. 2002. Lack of a pheromonal sense in phytosaurs and other archosaurs, and its implications for reproductive communication. Paleobiology 28:544–550.
Sereno PC. 1991. Lesothosaurus, "Fabrosaurids," and the early evolution of Ornithischia. J Vert Paleontol 11:168–197.
Sereno PC, Wilson JA, Conrad JL. 2004. New dinosaurs link southern landmasses in the Mid-Cretaceous. Proc R Soc Lond B 271: 1325–1333.
Snively E, Cotton JR, Ridgely RC, Witmer LM. 2013. Multibody dynamics model of head and neck function in Allosaurus (Dinosauria, Theropoda). 2013. Paleontol Electron 16:11A–22A. palaeo-electronica.org/content/2013/389-allosaurus-feeding.
Soares D. 2002. An ancient sensory organ in crocodilians. Nature 417:241–242.
Spotila JR, Terpin KM, Dodson P. 1977. Mouth gaping as an effective thermoregulatory device in alligators. Nature 265:235–236.
Spray DC, Belkin DB. 1973. Thermal patterns in the heating and cooling of *Iguana iguana* and *Ctenosaura hemilopha*. Comp Biochem Physiol 44A:881–892.
Sullivan RM. 2003. Revision of the dinosaur *Stegoceras Lambe* (Ornithischia, Pachycephalosauridae). J Vertr Paleontol 23: 181–207.
Symonds MR, Elgar MA. 2013. The evolution of body size, antennal size and host use in parasitoid wasps (Hymenoptera: Chalcidoidea): a phylogenetic comparative analysis. PLoS One 8:e78297.
Tattersall GJ, Cadena V, Skinner MC. 2006. Respiratory cooling and thermoregulatory coupling in reptiles. Resp Physiol Neurobiol 154: 302–318.
Taylor MP. 2010. Sauropod dinosaur research: a historical review. Geol Soc Lond Spec Publ 343:361–386.
Therrien F, Henderson DM. 2007. My theropod is bigger than yours … or not: estimating body size from skull length in theropods. J Vert Paleontol 27:108–115.

Thompson RS, Parish JC, Maidment SC, Barrett PM. 2012. Phylogeny of the ankylosaurian dinosaurs (Ornithischia: Thyreophora). J Syst Palaeontol 10:301–312.
Tschopp E, Mateus O, Benson RBJ. 2015. A specimen-level phylogenetic analysis and taxonomic revision of Diplodocidae (Dinosauria, Sauropoda). PeerJ 3:e857.
Upchurch P. 1999. The phylogenetic relationships of the Nemegtosauridae (Saurischia, Sauropoda). J Vert Paleontol 19:106–125.
Verwaijen D, Van Damme R, Herrel A. 2002. Relationships between head size, bite force, prey handling efficiency and diet in two sympatric lacertid lizards. Funct Ecol 16:842–850.
von Düring M. 1973. The ultrastructure of lamellated mechanoreceptors in the skin of reptiles. Anat Embryol 143:81–94.
von Düring M. 1974. The ultrastructure of cutaneous receptors in the skin of *Caiman crocodilus*. In Symposium Mechanoreception. VS Verlag für Sozialwissenschaften. p. 123–134.
von Düring M, Miller MR. 1979. Sensory nerve endings in the skin and deeper structures. In: Gans C, Northcutt RG, Ulinski P, editors. *Biology of the Reptilia, 9. Neurology A*. New York: Academic Press. p 407–442.
Watanabe A, Slice DE. 2014. The utility of cranial ontogeny for phylogenetic inference: a case study in crocodylians using geometric morphometrics. J Evol Biol 27:1078–1092.
Weishampel DB, Dodson P, Osmólska H. 2004. *The Dinosauria*. Berkeley, Los Angeles, London: University of California Press.
Wheeler PE. 1978. Elaborate CNS cooling structures in large dinosaurs. Nature 275:441–443.
Wilson JA. 2005. Redescription of the Mongolian sauropod *Nemegtosaurus mongoliensis* Nowinski (Dinosauria: Saurischia) and comments on Late Cretaceous sauropod diversity. J Syst Palaeontol 3:283–318.
Wilson JA, Sereno PC. 1998. Early evolution and higher-level phylogeny of sauropod dinosaurs. J Vert Paleontol 18:1–79.
Witmer LM. 1995. Homology of facial structures in extant archosaurs (Birds and Crocodilians), with special reference to paranasal pneumaticity and nasal conchae. J Morphol 225:269–327.
Witmer LM. 1997. The evolution of the antorbital cavity of archosaurs: a study in soft-tissue reconstruction in the fossil record with an analysis of the function of pneumaticity. J Vert Paleontol 17:1–76.
Witmer LM. 2001. Nostril position in dinosaurs and other vertebrates and its significance for nasal function. Science 293:850–853.
Witmer LM, Ridgely RC. 2008. The paranasal air sinuses of predatory and armored dinosaurs (Archosauria: Theropoda and Ankylosauria) and their contribution to cephalic structure. Anat Rec 291:1362–1388.
Witmer LM, Ridgely RC. 2009. New insights into the brain, braincase, and ear region of *Tyrannosaurus* (Dinosauria, Theropoda), with implications for sensory organization and behavior. Anat Rec 292:1266–1296.
Witmer LM, Ridgely RC, Dufeau DL, Semones MC. 2008. Using CT to peer into the past: 3D visualization of the brain and ear regions of birds, crocodiles, and nonavian dinosaurs. In: Endo H, Frey R, editors. *Anatomical imaging: towards a new morphology*. Tokyo: Springer-Verlag. p 67–88.
Wold S, Ruhe A, Wold H, Dunn WJ. 1984. The collinearity problem in linear regression. The partial least squares (PLS) approach to generalized inverses. SIAM J Sci Comput 5:735–743.
Woodruff DC, Foster JR. 2017. The first specimen of *Camarasaurus* (Dinosauria:Sauropoda) from Montana: the northernmost occurrence of the genus. PLoS ONE 12:e0177423.
Yeomans KA, Golder PA. 1982. The Guttman-Kaiser criterion as a predictor of the number of common factors. Statistician 31:221–229.
You HL, Tanoue K, Dodson P. 2008. New data on cranial anatomy of the ceratopsian dinosaur *Psittacosaurus major*. Acta Palaeontol Pol 53:183–196.